Evaluation of Ultimate Strength of Stiffened Panels Under Longitudinal Thrust

Satoyuki Tanaka[a], Daisuke Yanagihara[b], Aya Yasuoka[a], Minoru Harada[c], Shigenobu Okazawa[a], Masahiko Fujikubo[d], Tetsuya Yao[e]

[a] *Graduate School of Engineering, Hiroshima University, Japan*
[b] *Graduate School of Science and Engineering, Ehime University, Japan*
[c] *Nippon Kaiji Kyokai, Japan*
[d] *Graduate School of Engineering, Osaka University, Japan*
[e] *Tsuneishi Shipbuilding Company Ltd., Japan*

Abstract

A series of collapse analyses is performed applying nonlinear FEM on stiffened panels subjected to longitudinal thrust. MSC.Marc is used. Numbers, types and sizes of stiffeners are varied and so slenderness ratio as well as aspect ratio of local panels partitioned by stiffeners keeping the spacing between adjacent longitudinal stiffeners the same. Initial deflection of a thin-horse mode is imposed on local panels and that of flexural buckling and tripping modes on stiffeners to represent actual initial deflection in stiffened panels in ship structures. On the basis of the calculated results, buckling/plastic collapse behaviour of stiffened panels under longitudinal thrust is investigated. The calculated ultimate strength are compared with those obtained by applying several existing methods such as CSR for bulk carriers and PULS. Simple formulas for stiffened panels, of which collapse is dominated fundamentally by the collapse of local panels between longitudinal stiffeners, are also examined if they accurately estimate the ultimate strength. Through comparison of the estimated results with the FEM results, it has been concluded that PULS and modified FYH formulas fundamentally give good estimation of the ultimate strength of stiffened panels under longitudinal thrust.

Keywords: stiffened panels, longitudinal thrust, buckling/plastic collapse, ultimate strength, nonlinear FEM analyses, simple formulas, CSR-B, PULS

1. INTRODUCTION

A ship's hull girder is subjected to longitudinal bending produced by distributed self-weights, cargo weights, buoyancy forces as well as wave forces and inertia forces. The longitudinal bending produces thrust load acting on deck and/or bottom plating. Longitudinal stiffeners are provided on deck and bottom plating to prevent the occurrence of buckling of large panels partitioned by longitudinal girders/bulkheads and transverse frames/bulkheads. Buckling/plastic collapse of deck or bottom plating as a stiffened panel results in overall collapse of a ship's hull girder. Because of this, many research works have been performed up to now to clarify buckling/plastic collapse behaviour and strength of stiffened panels subjected to various loads [1-7].

The number of stiffeners and the aspect ratio of the local panel partitioned by stiffeners are similar depending on the types and sizes of ships. For example, bottom plating of Handy-size bulk carrier has, in general, two longitudinal stiffeners and the aspect ratio as a stiffened panel partitioned by girders and floors is around 1. Consequently, aspect ratio of the local panel partitioned by longitudinal stiffeners is around 3. The aspect ratio of the local panel is almost the same even for Cape-size bulk carrier, but the number of longitudinal stiffeners between girders increases to five or six. In this case, aspect ratio of the stiffened panel between girders becomes around 0.5. On the other hand, at deck plating of VLCC, the aspect ratio of the stiffened panel between longitudinal bulkheads is around 0.2 and the number of longitudinal stiffeners is, for example, twenty-five. When buckling/plastic collapse behaviour of stiffened panels is dominated by local buckling of the panels or stiffeners, the ultimate strength may be almost the same regardless of the number of stiffeners. This is the case of an ordinary ship structure since size and number of stiffeners are so determined that the stiffened panel does not undergo overall buckling. On the other hand, when overall buckling of stiffened panel takes place as the primary buckling, the stiffening effect of the stiffeners varies in accordance with the number of stiffeners. It is then supposed that the buckling/plastic collapse behaviour and the ultimate strength are influenced by the numbers and slenderness ratio of stiffeners as well as on the slenderness ratio of local panels. However, as mentioned above, such collapse is not common in real ship structures and shall not be discussed in detail.

In recent years, large-scaled computer simulation applying nonlinear FEM has become possible owing to the development in computer hardwares and softwares. In this study, a series of nonlinear FEM analyses is performed to simulate buckling/plastic collapse behaviour of stiffened panels and to evaluate their ultimate strength under longitudinal thrust.

Common Structural Rules came into effect in 2006 for bulk carriers (CSR-B) [8] and double hull oil tankers (CSR-T)) [9], respectively, as design standards for ship structures. They include formulas and calculation methods to evaluate structural strength such as yielding, bucking and ultimate strength of panels and stiffened panels as well as hull girders. In CSR-B, ultimate strength of panels and stiffened panels are evaluated by formulas in Section 3, Chapter 6. For stiffened panel, buckling collapse of local panels, buckling collapse of stiffened panels and torsional buckling collapse of stiffeners are considered as possible collapse modes. Among the ultimate strength for individual collapse modes, the lowest is considered as the real ultimate strength. On the other hand, in CSR-T, the use of PULS [10] is recommended for evaluation of the ultimate strength of panels and stiffened panels. PULS is on the basis of research works by Byklum and Amdahl [11], Byklum *et al.* [12] and Steen *et al.* [13, 14]. In PULS, elastic large deflection analysis is performed assuming deflection modes of local and overall buckling independently. The ultimate strength is determined as the lowest initial yielding strength in terms of membrane equivalent stresses at selected several points in the model. PULS is recognised as an effective method to evaluate the ultimate strength. However, the software is not opened and is a black box, although its fundamental idea can be seen in Refs. [11 - 14].

On the other hand, Fujikubo *et al.* [15, 16] proposed a simple method to evaluate the ultimate strength of stiffened panels subjected to longitudinal thrust. Their method is extended for stiffened panels subjected to combined bi-axial thrust and lateral pressure [17 - 21]. In their methods, a continuous stiffened panel with many stiffeners is the target structure and the stiffened panel is modelled as a stiffener with attached plating. It is assumed that local panel between longitudinal stiffeners can collapse before overall buckling of a stiffened panel takes place. Elastic large deflection analysis is performed in an analytical manner on this beam-column model of a stiffener with attached plating. The ultimate strength is determined as the lowest initial yielding strength evaluated at several selected points. It was confirmed that this

method gives relatively accurate ultimate strength through comparison of the calculated results with those by the nonlinear FEM analysis. However, numerical iterative calculation is required in this method. This method is hereafter called Fujikubo/Yanagihara's method (FY method).

Harada [17] and Harada *et al.* [18 - 21] proposed a set of closed-form formulas for evaluation of the ultimate strength of stiffened panels subjected to combined bi-axial thrust and lateral pressure introducing some assumptions to FY method. These formulas are hereafter called FYH (Fujikubo/Yanagihara/Harada) formulas.

In this paper, a series of nonlinear FEM analyses is firstly performed on stiffened panels with longitudinal stiffeners of various numbers, types and sizes. Slenderness ratio and aspect ratio of the local panels partitioned by stiffeners are also varied, but the spacing between longitudinal stiffeners is kept the same. MSC.Marc [22] is used for analysis to apply longitudinal thrust on stiffened panels. Initial deflection of a thin-horse mode is imposed on local panels whereas that of flexural buckling and tripping modes on longitudinal stiffeners. Influence of welding residual stress is not considered in the present analyses. On the basis of the calculated results, buckling/plastic collapse behaviour of stiffened panels under longitudinal thrust is investigated.

Then, some existing methods to evaluate the ultimate strength of stiffened panels subjected to longitudinal thrust are briefly explained. They are PULS, CSR-B, FY method and FYH formulas. The calculated results by these methods are compared with nonlinear FEM results. Through comparison of the calculated results, existing methods of calculation are assessed.

2. NONLINEAR FEM ANALYSES ON STIFFENED PANELS

2.1. Stiffened panels for nonlinear FEM analysis

As fundamental models, stiffened panels from bottom plating of bulk carrier and deck plating of VLCC are selected. The schematic illustration of the model is shown in Fig.1 together with the extent of modelling. Longitudinal girders and transverse frames are provided on plating, and two longitudinal stiffeners exist between adjacent longitudinal girders in this drawing. The

spacing between adjacent transverse frames is denoted as a and that between adjacent longitudinal girders as B. The spacing between adjacent longitudinal stiffeners is denoted as b.

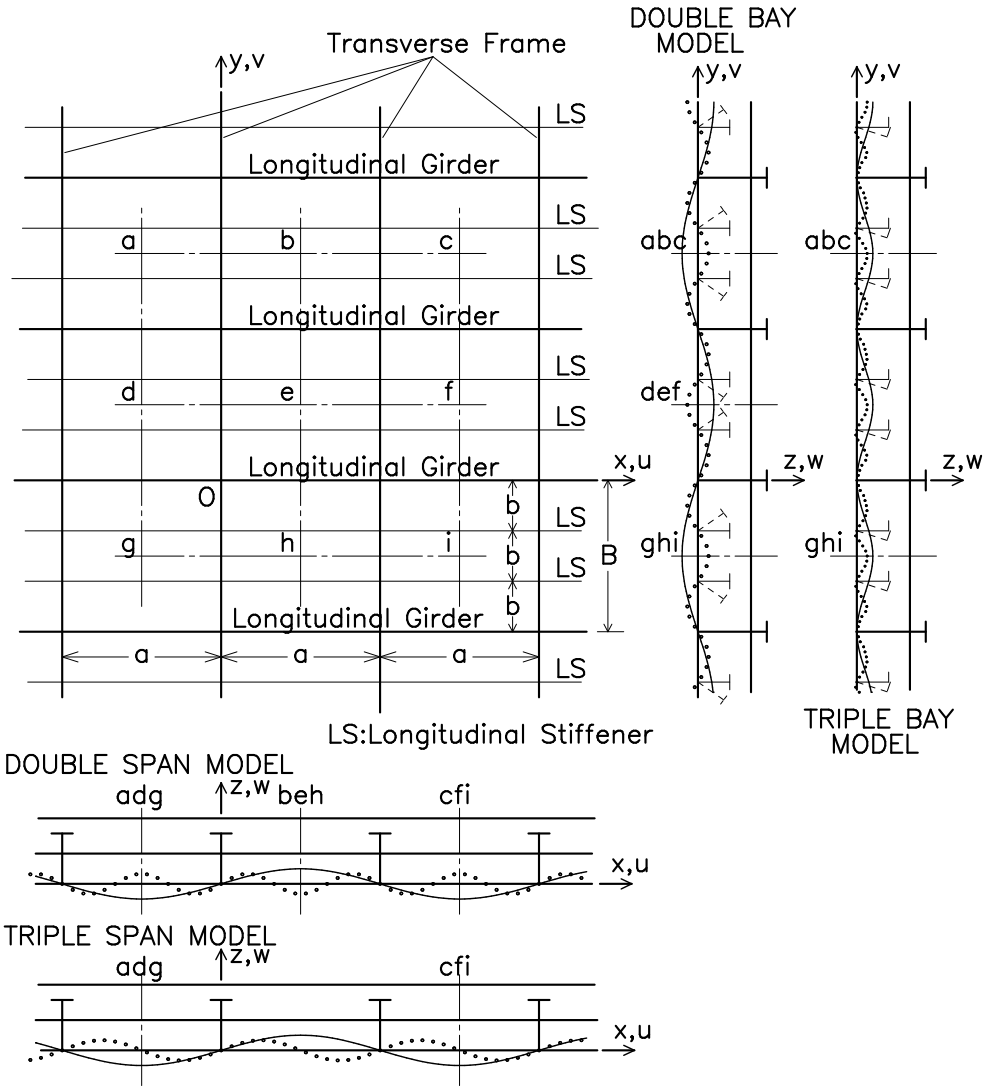

Figure 1: Typical stiffened panel in ship structure and its modelling extent

For bulk carrier model, aspect ratio of the local panel is taken as $a/b = 3.0$, and that for VLCC model as $a/b = 5.0$. A local panel ($a \times b$) is defined

as a part of stiffened panel partitioned by longitudinal girders/stiffeners and transverse frames. Six thicknesses are selected for each aspect ratio of the local panel, within which range the thicknesses of existing ships may be included. The assumed dimensions of the local panels are as follows:

- Bulk carrier model:
  $a \times b = 2,550 \times 850$mm $(a/b = 3.0)$
  $t_p = 33, 22, 16, 13, 11, 9.5$mm
  $\beta = (1.01), (1.51), (2.07), (2.55), (3.02), (3.49)$

- VLCC model:
  $a \times b = 4,750 \times 950$mm $(a/b = 5.0)$
  $t_p = 37, 25, 18.5, 15, 12.5, 11$mm
  $\beta = (1.00), (1.48), (2.00), (2.47), (2.97), (3.37)$

where t_p is a thickness of local panel partitioned by stiffeners, and β is its slenderness ratio, which is defined as:

$$\beta = \frac{b}{t_p}\sqrt{\frac{\sigma_Y}{E}} \tag{1}$$

σ_Y and E are yield stress and Young's modulus of the material, respectively. It is known that the thicknesses defined above give slenderness ratios which are roughly equal to β =1.0, 1.5, 2.0, 2.5, 3.0 and 3.5, respectively.

As for stiffeners, flat-bar, angle-bar and tee-bar stiffeners are selected. Their shapes are shown in the illustration attached to Table 1 together with definition of height, breadth and thicknesses. Four sizes of stiffeners are considered for each type, which are denoted as S1, S2, S3 and S4. Dimensions of the stiffeners are summarised in Table 1.

The calculation models are denoted as "pqSrBs", where
- "p" stands for type of stiffener
  $p = F$: Flat-bar; $p = A$: Angle-bar; $p = T$: Tee-bar
- "q" stands for aspect ratio of local panel
  $q = 3$: $a/b = 3.0$; $q = 5$: $a/b = 5.0$
- "r" stands for size of stiffener
  $r = 1$: S1-size; $r = 2$: S2-size; $r = 3$: S3-size; $r = 4$: S4-size
- "s" stands for slenderness ratio of local panel

$s = 10$: $\beta = 1.0$; $s = 15$: $\beta = 1.5$; $s = 20$: $\beta = 2.0$;
$s = 25$: $\beta = 2.5$; $s = 30$: $\beta = 3.0$; $s = 35$: $\beta = 3.5$

For example, "A5S2B30" stands for stiffened panel with angle-bar stiffener of S2 size of which local panel has aspect ratio of 5.0 and slenderness ratio of 3.0. Keeping the size ($a \times b$) of the local panel unchanged, number of stiffeners is varied as 1, 2, 4, 8 and infinity.

Table 1: Types and sizes of stiffeners

Size	Flat-bar	Angle-bar	Tee-bar
S1	150×17	$150 \times 90 \times 9/12$	$138 \times 9{+}90 \times 12$
S2	250×25	$250 \times 90 \times 10/15$	$235 \times 10{+}90 \times 15$
S3	350×35	$400 \times 100 \times 12/17$	$383 \times 12{+}100 \times 17$
S4	500×35	$600 \times 150 \times 15/20$	$580 \times 15{+}150 \times 20$

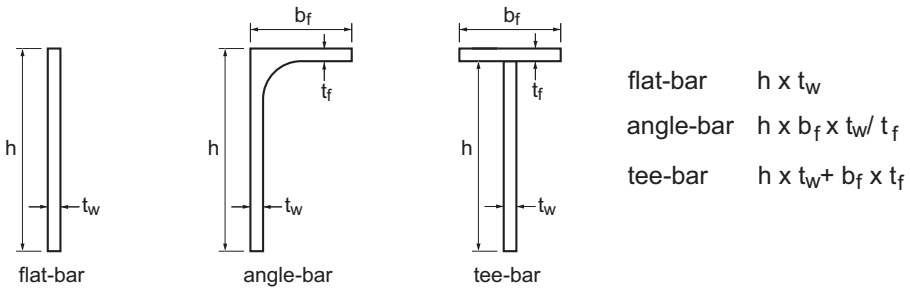

In summary, as for local panels, two aspect ratios and six slenderness ratios are considered, and as for stiffeners, three types, four sizes and five numbers. Thus, number of calculated models is altogether 720 ($= 2 \times 6 \times 3 \times 4 \times 5$).

2.2. Modelling of stiffened panels for nonlinear FEM analyses [23]

Lateral deflection of stiffened panel can be represented as a sum of the deflection components of local panel buckling mode and overall buckling mode, which are indicated in Fig.1 by dotted lines and solid lines, respectively.

2.2.1. Extent of modelling in longitudinal direction

When number of half-waves in local panel buckling mode in longitudinal direction is odd, the modelling extent in the longitudinal direction can be adg-beh or beh-cfi imposing symmetry condition on the boundary, which is expressed as:

$$\begin{cases} u: \text{ uniform along adg, beh and cfi} \\ \theta_y = \theta_z = 0 \end{cases} \tag{2}$$

This model is called as 1/2 + 1/2 span model.

On the other hand, when number of half-waves in local panel buckling mode in longitudinal direction is even, the modelling extent in the longitudinal direction has to be adg-cfi imposing periodic condition expressed as follows.

$$\begin{cases} u: \text{uniform along adg and cfi} \\ v_{adg} = v_{cfi}, \quad w_{adg} = w_{cfi} \\ \theta_{xadg} = \theta_{xcfi}, \quad \theta_{yadg} = \theta_{ycfi}, \quad \theta_{zadg} = \theta_{zcfi} \end{cases} \tag{3}$$

This model is called as 1/2 + 1 + 1/2 span model.

2.2.2. Extent of modelling in transverse direction

Also for the extent of modelling in the transverse direction, there exist two modellings, which are 1/2 + 1/2 bay model (abc-def or def-ghi) and 1/2 + 1 + 1/2 bay model (abc-ghi).

When stiffeners have symmetry cross-section as flat-bar or tee-bar, 1/2 + 1/2 bay model can be used. On the other hand, when cross-section of a stiffener is not symmetry and lateral pressure loads act in addition to the thrust load, deflection of a local panel or a whole stiffened panel becomes not symmetric along their centre lines. In this case, 1/2 + 1 + 1/2 bay model has to be used. As for the extent of modelling including the case of shear loading, more general discussion is made by Xu *et al.* [24].

The boundary condition of 1/2 + 1/2 bay model is a symmetry condition, which is expressed as:

$$\begin{cases} v: \text{ uniform along abc, def and ghi} \\ \theta_x = \theta_z = 0 \end{cases} \tag{4}$$

For 1/2 + 1 + 1/2 bay model, periodic condition is necessary as follows.

$$\begin{cases} u_{abc} = u_{ghi}, \quad w_{abc} = w_{ghi} \\ v: \text{uniform along abc and ghi} \\ \theta_{xabc} = \theta_{xghi}, \quad \theta_{yabc} = \theta_{yghi}, \quad \theta_{zabc} = \theta_{zghi} \end{cases} \tag{5}$$

2.2.3. Modelling in the present analysis

In the present analysis, (1/2 + 1 + 1/2 span)/(1/2 + 1 + 1/2 bay) model is used for stiffened panels with two, four and eight stiffeners. Such a model is called by the authors as triple span/triple bay model.

When number of stiffeners is infinite, (1/2 + 1 + 1/2 span)/(1/2 + 1 + 1/2 bay) model is also used. In this case, longitudinal girder is not considered. On the other hand, when number of stiffener is one, (1/2 + 1 + 1/2 span)/(1 + 1 full bay) model is used.

Figures 2 (a), (b) and (c) show stiffened panels with one stiffener, infinite number of stiffeners and four stiffeners, respectively. Models are accompanied by initial deflection, which shall be explained later in *2.3*.

Longitudinal girders and transverse frames are not modelled, but the panel is assumed to be simply supported along the lines of their attachment. In general, webs of longitudinal girders or transverse frames resist against the rotation of local panel along their intersection lines when lateral deflection is produced in the local panel. This interaction increases the buckling strength of local panels and so their ultimate strength. In the present modelling, however, this influence is ignored, which shall result in the lower buckling strength and ultimate strength. Stiffener's web is also assumed to be simply supported in the horizontal direction along the intersection lines with web of transverse frames. At the same time, stiffener's web is assumed to keep a right angle with local panel along their intersection lines. MPC (Multiple Point Constraint) condition is imposed for displacements along the boundary cross-sections where periodic conditions are imposed.

The material is assumed to be elastic/perfectly plastic. Material properties assumed in the analyses are as follows:

Yield stress:	$\sigma_Y = 313.6$ MPa
Young's modulus:	$E = 205.8$ GPa
Poisson's ratio:	$\nu = 0.3$
Strain hardening rate:	$H' = 0$

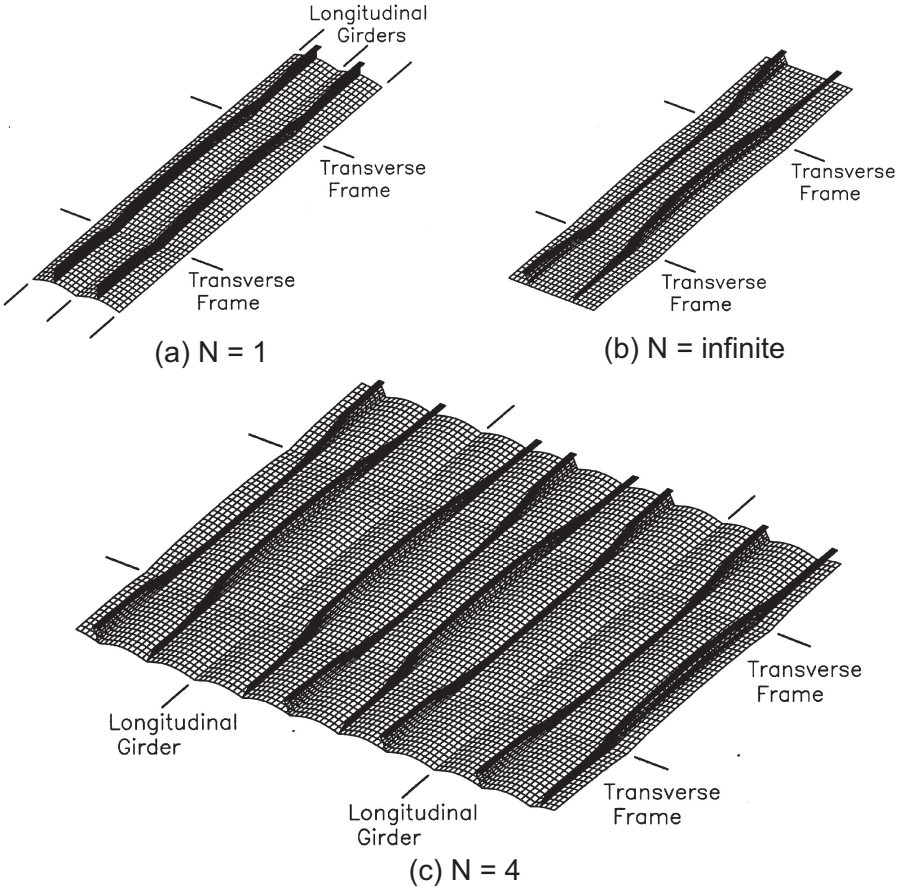

Figure 2: Typical FEM models of stiffened panels with initial deflection

2.3. FEM analysis

A series of elastoplastic large deflection analyses is performed using the nonlinear FEM code, MSC.Marc [22]. Bilinear shell element (Element No.

75) is used. This element is a four-noded thick-shell element with three translations and three rotations per node as degrees of freedom. Shear deformation in the thickness direction is considered in this element. Eleven integration points are provided towards thickness direction. Meshing of the local panel is the same regardless of the aspect ratio, and one half-wave region of the elastic buckling mode is represented by 10×10 elements. Stiffener web and flange are divided into six elements towards its depth and breadth directions, respectively. This division is the same regardless of the stiffener size. FEM meshing for T3S4B35 is shown in Figs.3 (a) and (b) together with a coordinate system. The translations are denoted as (u, v, w) and the rotations as $(\theta_x, \theta_y, \theta_z)$, which are indicated in the figure.

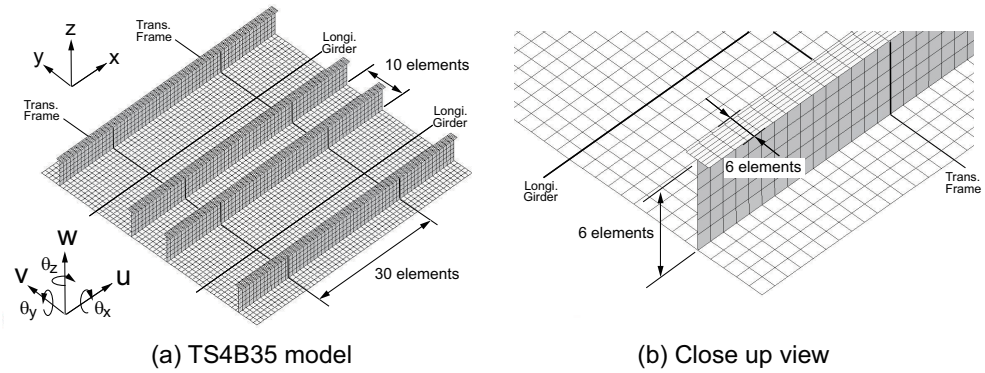

Figure 3: Meshing of FEM stiffened panel

The nonlinear FEM calculation performed in the present paper is a part of comprehensive calculations carried out in the research committee established in The Japan Society of Naval Architects and Ocean Engineers [25] to examine the ultimate strength formulas in the newly proposed ISO standards. In the committee calculation, three nonlinear FEM codes were used including in-house codes. It was confirmed that the differences between ultimate strength by different codes including MSC.Marc are very small.

2.4. Initial deflection in FEM model

The mode and magnitude of initial deflection were measured in 33 local panels partitioned by stiffeners at deck plating of bulk carrier and pure car carrier [26]. Similar measurement was carried out on inner bottom plating

of bulk carrier in 45 local panels and 30 longitudinal stiffeners [27]. It was found that initial deflection in local panels is of a thin-horse mode in almost all cases when heat treatment was not carried out after welding to remove excess initial deflection. Here, thin-horse mode indicates the mode just like a breast of a thin horse with convex skin between ribs. On the basis of the measured results, it is assumed that the initial deflection consists of three components, which are (i) overall buckling mode in stiffened panel; (ii) overall buckling and tripping modes in stiffeners; and (iii) thin-horse mode in local panels between stiffeners, see Figs.4 (a), (b) and (c).

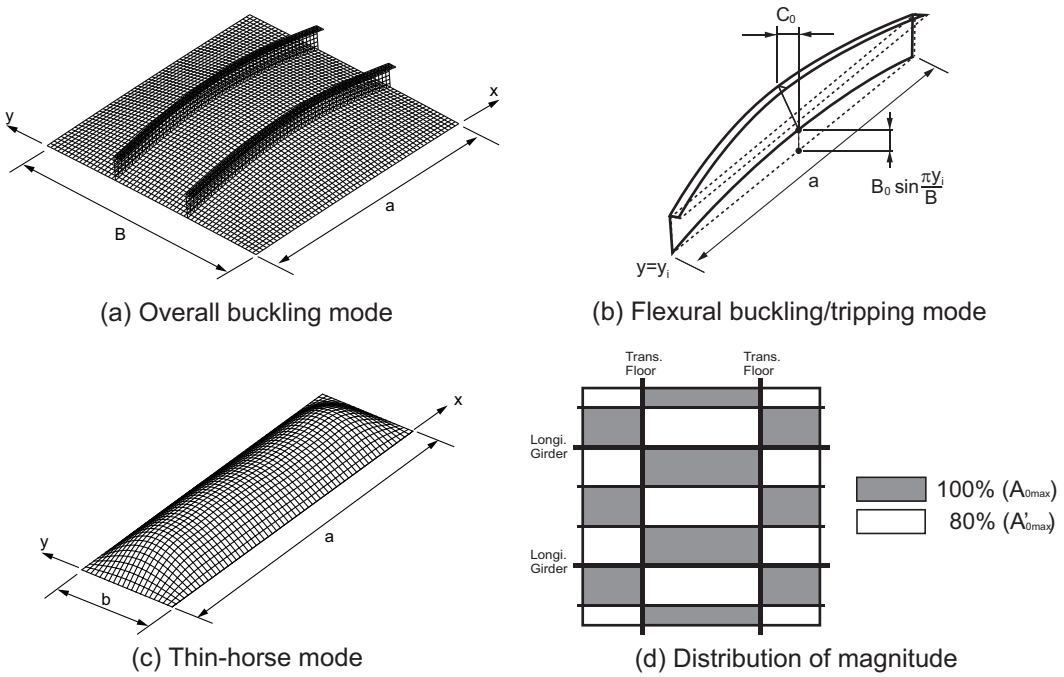

Figure 4: Assumed initial deflection in stiffened panel

As for the initial deflection in longitudinal stiffeners, measured results in Ref. [27] indicate that initial deflection of a flexural buckling mode is in an opposite direction at seven locations among measured twenty boundaries of adjacent spans. Regarding initial deflection of stiffeners in a horizontal direction (tripping mode), they are in an opposite direction at four locations among twenty. However, the direction of initial deflection in the adjacent spans is set as opposite. This is because the buckling/ultimate strength

is lower when initial deflections in the adjacent spans are in an opposite direction compared to the case of the same direction. Thus, initial deflection of an overall buckling mode in stiffened panel is expressed as:

$$w_{0ov} = B_0 \sin\frac{\pi x}{a} \sin\frac{\pi y}{B} \tag{6}$$

The origin of the coordinate system is taken at an intersection point of a longitudinal girder and a transverse frame, see point O in Fig.1.

Then, initial deflection of the i-th longitudinal stiffener located at $y = y_i$ is expressed as follows.

$$w_{0si} = B_0 \sin\frac{\pi x}{a} \sin\frac{\pi y_i}{B} \tag{7}$$

Initial deflection of a tripping mode is expressed as:

$$v_{0si} = C_0 \frac{z}{h_s} \sin\frac{\pi x}{a} \tag{8}$$

where $h_s = t_p/2 + h$ and z is measured from the mid-thickness plane of the panel.

On the other hand, initial deflection of a thin-horse mode in local panel is expressed as follows.

$$w_{0thin} = \left| A_{0max} \sum_{m=1}^{11} A_{0m} \sin\frac{m\pi x}{a} \sin\frac{\pi y}{b} \right| \tag{9}$$

Consequently, initial deflection in panel is expressed as the sum of deflections of an overall mode and of a thin-horse mode as follows.

$$\begin{aligned} w_{0p} = w_{0ov} + w_{0thin} &= B_0 \sin\frac{\pi x}{a} \sin\frac{\pi y}{B} \\ &+ \left| A_{0max} \sum_{m=1}^{11} A_{0m} \sin\frac{m\pi x}{a} \sin\frac{\pi y}{b} \right| \end{aligned} \tag{10}$$

Measured results indicate that B_0 lies in the range of -0.0007a and 0.0006a and C_0 in the range of -0.00125a and 0.00135a, respectively [27]. In the present analyses, B_0 and C_0 are assumed as follows.

$$B_0 = C_0 = 0.001 \times a \tag{11}$$

As for the initial deflection of a thin-horse mode in local panel expressed by Eq.(9) or the second term in Eq.(10), deflection components given in Table 2 are used. They are the coefficients of idealised initial deflection based on the measured results [26].

As for the initial deflection in local panels, buckling mode is sometimes assumed for the collapse analysis with the measured maximum magnitude. However, such initial deflection is unrealistic and gives too low ultimate strength. Even if the plate is accompanied with initial deflection of a thin-horse mode, the plate buckles in buckling mode, and the post-buckling behaviour is ruled by the magnitude of deflection component of the buckling mode in initial deflection and not by the maximum magnitude of initial deflection [26].

Table 2: Coefficients making initial deflection of thin-horse mode

Aspect ratio	A_{01}	A_{02}	A_{03}	A_{04}	A_{05}	A_{06}
$a/b = 3.0$	1.1458	−0.0616	0.3079	0.0229	0.1146	−0.0065
$a/b = 5.0$	1.1271	−0.0697	0.3483	0.0375	0.1787	−0.0199

Aspect ratio	A_{07}	A_{08}	A_{09}	A_{10}	A_{11}
$a/b = 3.0$	0.0327	0.0000	0.0000	−0.0015	−0.0074
$a/b = 5.0$	0.0995	0.0107	0.0537	−0.0051	0.0256

Coefficients of initial deflection $A_{0m}(m = 1, \cdots, 11)$ in Table 2 makes initial deflection of a thin-horse mode of which maximum magnitude is very near to 1.0. Then, maximum magnitude of initial deflection of a thin-horse mode, A_{0max}, is assumed to be:

$$A_{0max} = \text{Smaller}[0.1\beta^2 t_p,\ 6 \text{ mm}] \tag{12}$$

where $0.1\beta^2 t_p$ is the magnitude of average initial deflection proposed by Smith *et al.* [28] based on the measured results, and 6 mm is the maximum allowable magnitude specified in Japan Shipbuilding Quality Standard (JSQS) [29]. In addition to this, 20 % difference is given in the magnitude of initial deflection

in the adjacent local panels alternatively as indicated in Fig.4 (d). That is, the maximum magnitude of initial deflection of non-shaded panels in Fig.4 (d) is set as:

$$A'_{0max} = 0.8 \times A_{0max} \tag{13}$$

This is to give irregularity in the initial deflection to obtain numerically stable solution.

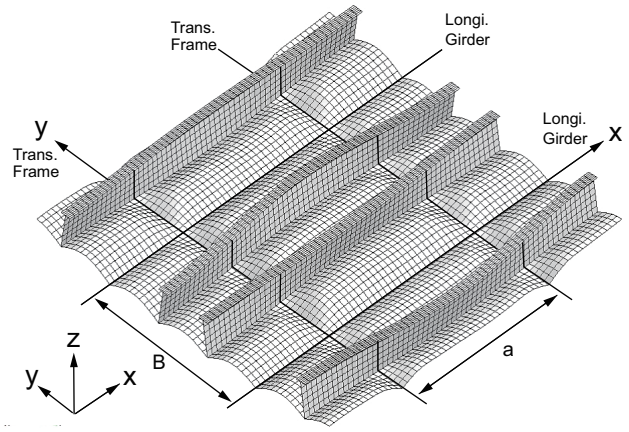

Figure 5: Initial deflection given on T3S4B35

When number of stiffeners is infinite, Eq.(7) reduces to:

$$w_{0s} = B_0 \sin \frac{\pi x}{a} \tag{14}$$

and so the first term of Eq.(10). In this case, initial deflection in local panel is represented as the sum of thin-horse mode (Eq.(9)) and overall buckling mode (Eq.(14)).

Figure 5 shows initial deflection of a typical stiffened panel model, T3S4B35. The initial deflection is magnified by fifty in this figure. Influence of welding residual stress is not considered in the present analysis.

3. CALCULATED RESULTS AND DISCUSSIONS

3.1. Ultimate strength and collapse behaviour of stiffened panels under longitudinal thrust

Ultimate strength of all together 720 cases are summarised in Figs.6 through 11. In each figure, ultimate strength obtained by nonlinear FEM analyses is plotted against slenderness ratio of the local panel between stiffeners with various marks for stiffened panels having 1, 2, 4, 8 and infinite number of stiffeners. Chain lines with a dot and with two dots are ultimate strength obtained by CSR-B and PULS, respectively. On the other hand, the broken lines are by FY method, and the dotted and solid lines represent the ultimate strength calculated by FYH formulas and modified FYH formulas, which are completely the same in case of stiffened panels with angle-bar and tee-bar stiffeners. It should be noticed that the slenderness ratio is not for stiffener but for local panels between stiffeners.

As mentioned before, the size of stiffeners in ship structures are so determined that the overall buckling does not take place as the primary buckling. Therefore, slenderness ratio of a stiffener with attached plating is not considered as a governing parameter although this plays an important role when overall buckling takes place. Actually in the present analysis, overall buckling occurs in some cases as shall be shown later. However, overall buckling as the primary buckling is out of interests of this paper, and shall not be discussed in detail in the following. So, slenderness ratio and aspect ratio of the local panels partitioned by stiffeners as well as type, size and number of stiffeners are considered as parameters for discussion. On the other hand, the overall buckling as the secondary buckling, which takes place after the local panel buckling has occurred, is considered in a simple method to evaluate the ultimate strength of stiffened panel, although a column's slenderness ratio is not explicitly considered as a governing parameter to rule the overall buckling.

Now, attention is firstly focused on the results of FEM analyses. Scatters of the FEM results are observed depending on the number of stiffeners when the size of stiffener is small and the aspect ratio of the local panel between stiffeners is low. In concrete, when the aspect ratio of local panel is 3.0, size 1 stiffeners are provided and the slenderness ratio of the local panel is below 2.5, scatter is seen in the ultimate strength depending on the number of

stiffeners. When the aspect ratio of the local panel is 5.0 and size 1 stiffeners are provided, scatter is observed depending on the number of stiffeners for all slenderness ratios. For the same case but size 2 stiffeners are provided, scatter is seen when the slenderness ratio of the local panel is below 2.5. These are the cases when overall buckling dominates the collapse behaviour. Contrary to this, when scatter is not observed in the ultimate strength with different number of stiffeners, buckling/plastic collapse of local panel between longitudinal stiffeners dominates the collapse behaviour, and the ultimate strength is almost the same regardless of the number of stiffeners.

Here, two typical cases are considered when the ultimate strength varies and does not vary depending on the number of stiffeners. As for the former example, T3S1B10 (stiffened panel with tee-bar stiffeners of size S1 are attached; slenderness ratio and aspect ratio of the local panel are β=1.0 and a/b =3.0, respectively) is selected, and as for the latter example, F3S2B25 (stiffened panel with flat-bar stiffeners of size S2 are attached; slenderness ratio and aspect ratio of the local panel are β=2.5 and a/b =3.0, respectively). Figures 12 (a) and (b) show respective average stress-average strain relationships. On the other hand, collapse modes for these two cases are shown in Figs.13 and 14, respectively, for the models with 1, 8 and infinite number of stiffeners.

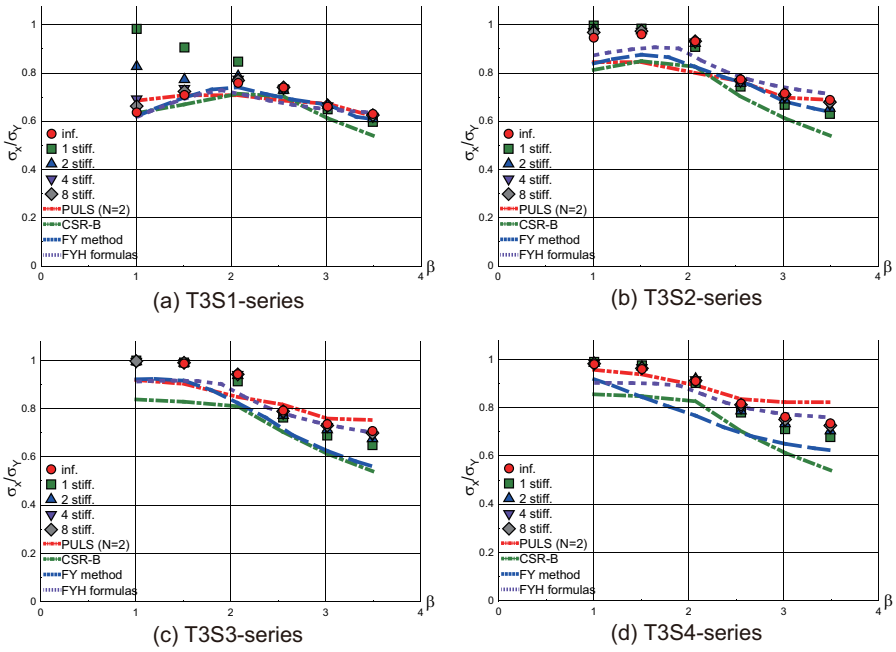

Figure 6: Ultimate strength of stiffened panels with tee-bar stiffeners (a/b=3.0)

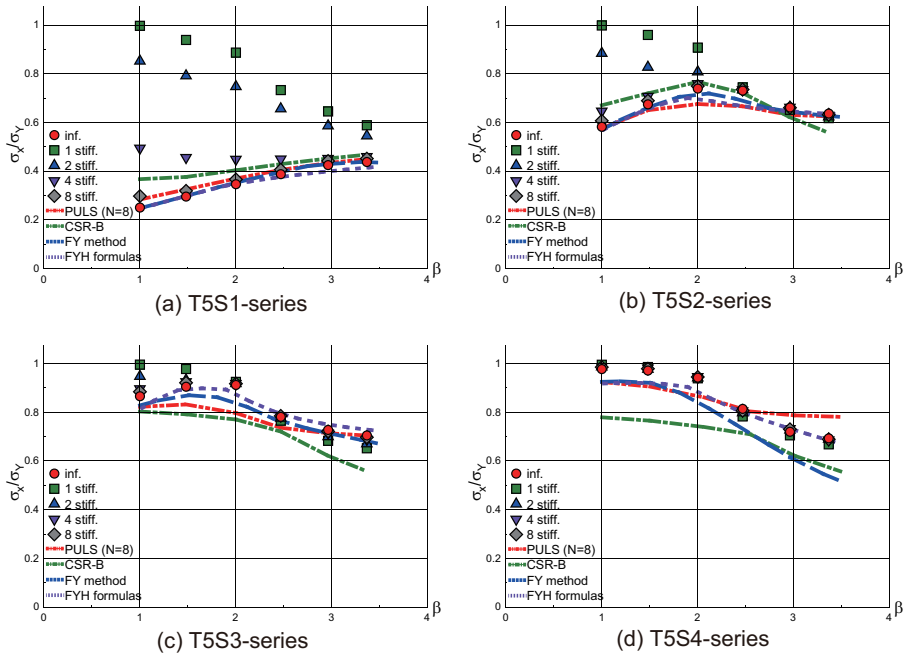

Figure 7: Ultimate strength of stiffened panels with tee-bar stiffeners (a/b=5.0)

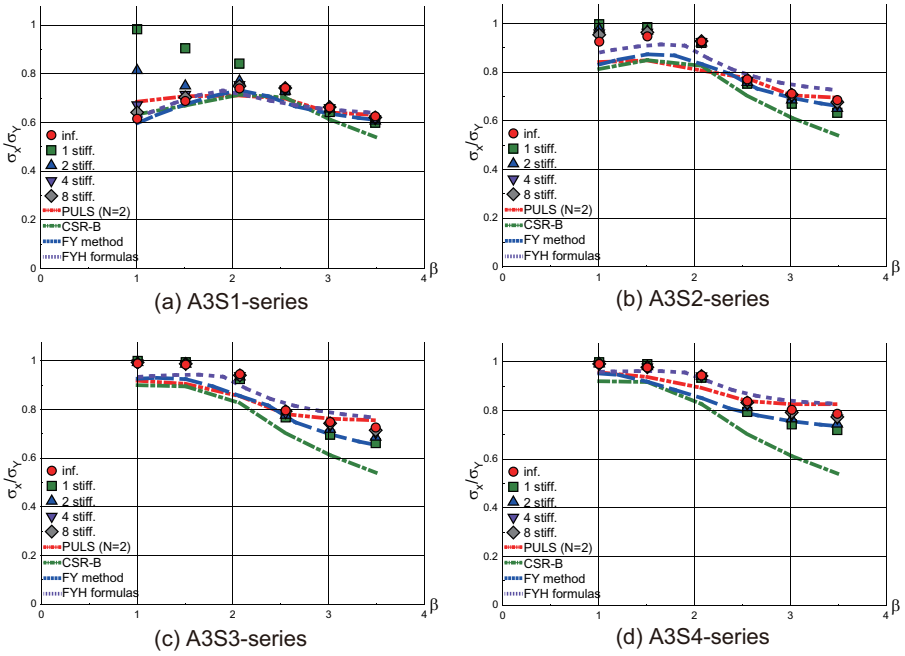

Figure 8: Ultimate strength of stiffened panels with angle-bar stiffeners (a/b=3.0)

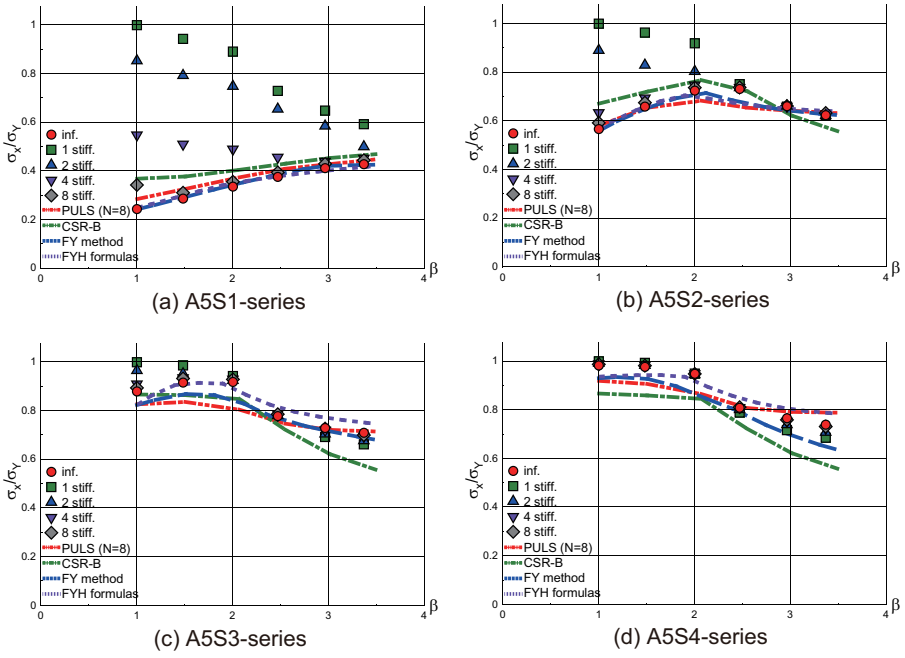

Figure 9: Ultimate strength of stiffened panels with angle-bar stiffeners (a/b=5.0)

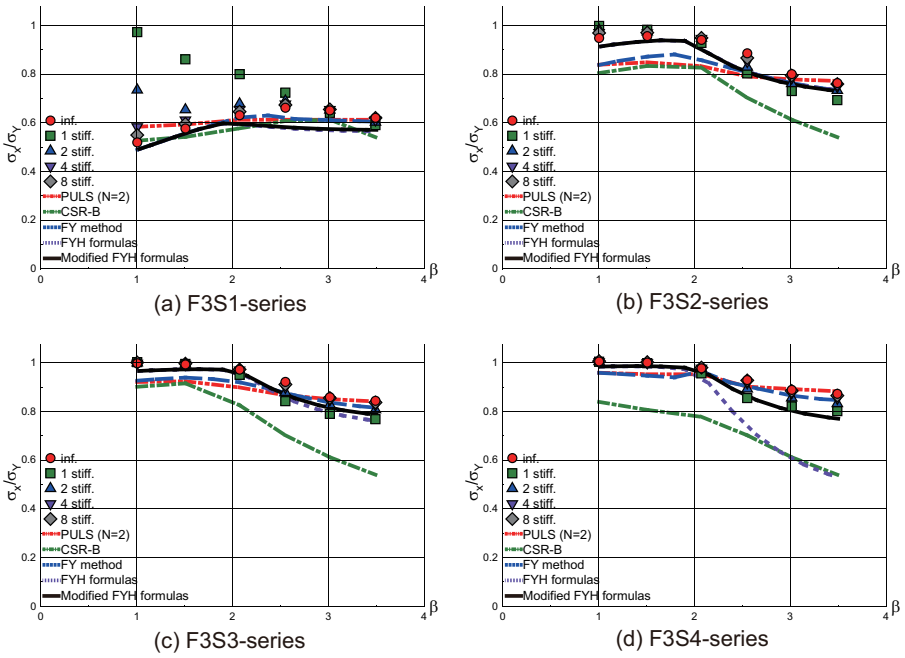

Figure 10: Ultimate strength of stiffened panels with flat-bar stiffeners (a/b=3.0)

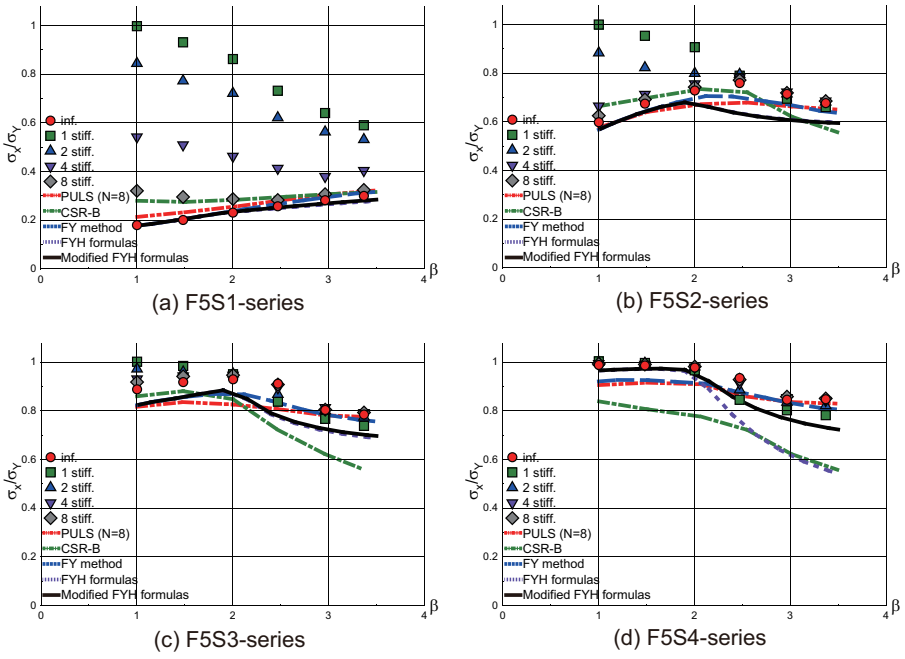

Figure 11: Ultimate strength of stiffened panels with flat-bar stiffeners (a/b=5.0)

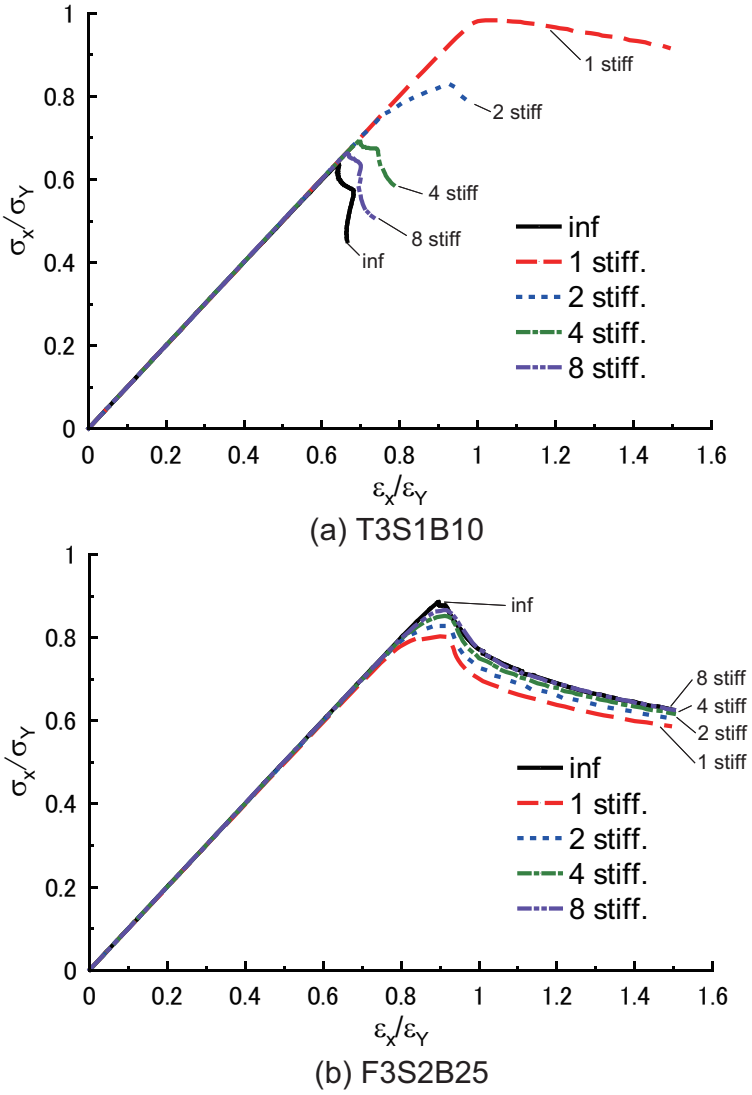

Figure 12: Average stress - Average strain curve

Figure 13 indicates that collapse is in an overall buckling mode regardless of the number of stiffeners. Overall buckling strength mainly depends on the aspect ratio of the whole stiffened panel and the panel thickness as well as size and number of stiffeners. When no stiffener is provided, overall buckling strength under simply supported condition is given as:

$$\sigma_E^p = \frac{\pi^2 E}{12(1-\nu^2)} \left(\frac{t_p}{B}\right)^2 \left(\frac{a}{B} + \frac{B}{a}\right)^2$$
$$= \frac{\pi^2 E}{12(1-\nu^2)} \left(\frac{t_p}{a}\right)^2 \left(1 + \frac{a^2}{B^2}\right)^2 \quad (15)$$

In the present model, local buckling strength is the same regardless of the number of stiffeners since the aspect ratio of all local panels between stiffeners and the stiffener spacing are kept the same. Contrary to this, overall buckling strength varies with the number of stiffeners because aspect ratio of the whole panel also varies as the number of stiffeners increases. The overall buckling strength, σ_E^p, ignoring stiffeners is given in Table 3. On the other hand, elastic buckling strength of stiffened panel, σ_E, is calculated applying FEM. Then, elastoplastic buckling strength performing plasticity correction by Johnson-Ostenfeld formula and the ultimate strength of the stiffened panel are also calculated and summarised in Table 3.

σ_E for stiffened panel with infinite number of stiffeners can be calculated as the buckling strength of a both-ends simply supported stiffener with attached plating, which results in $\sigma_E/\sigma_Y = 1.2745$. This is 8% higher than the FEM result shown in Table 3.

Firstly, the effect of stiffeners on buckling strength is known by comparing two elastic buckling strength, σ_E^p and σ_E. The last column of Table 3 indicates that the increasing effect of stiffeners on buckling strength increases as the number of stiffeners increases. Secondly, it is also seen that the elastoplastic buckling strength obtained by plasticity correction is in general lower than the ultimate strength when number of stiffeners is more than one.

In all cases, as indicated in Figs.13 (a), (b) and (c), stiffened panels collapse by the occurrence of overall buckling. In the post-ultimate strength range after overall buckling has taken place, stiffeners which locate in the compression side of overall bending undergoes tripping near the mid-span point of the stiffeners.

On the other hand, Figs.14 (a), (b) and (c) indicate that, panel collapses by local buckling and plastic deformation is concentrated at the mid-span region of local panels in the centre span of the model in case of F3S2B25

Table 3: Buckling and ultimate strength of stiffened panel (T3S1B10)

N	σ_E^p/σ_Y	σ_E/σ_Y	σ_{cr}/σ_Y	σ_u/σ_Y
1	1.1845	2.0750	0.8785	0.9831
2	0.4486	1.4465	0.8272	0.8271
4	0.2074	1.2452	0.7992	0.6927
8	0.1384	1.1921	0.7903	0.6627
inf.	0.1020	1.1756	0.7874	0.6370

N: number of stiffeners
σ_E^p: elastic buckling strength of panel without stiffeners (Eq.(15))
σ_E: elastic buckling strength of stiffened panel (FEM)
σ_{cr}: elastoplastic buckling strength of stiffened panel (Johnson-Ostenfeld correction)

$$\sigma_{cr} = (1 - \sigma_Y/4\sigma_E)\sigma_Y$$

σ_u: ultimate strength of stiffened panel (FEM)
σ_Y: yield stress of material

model. The collapse is dominated by local collapse of panel, although overall bending deformation takes place in stiffeners beyond the ultimate strength. Such collapse is denoted as plate-induced failure, while collapse of T3S1B10 is denoted as stiffener-induced failure. When plate-induced failure takes place, the ultimate strength is almost the same regardless of the number of stiffeners when the size of the local panel between longitudinal stiffeners is the same.

3.2. Ultimate strength by PULS

The ultimate strength evaluated by PULS [10] is plotted by chain lines with two dots in Figs.6 through 11. PULS can be applied to stiffened panels with any number of stiffeners. In these figures, however, number of stiffeners is taken as two and eight for stiffened panels of which local panels have aspect ratio, a/b, of 3 and 5, respectively. This is just to avoid that too many marks appear in the figures. So, when PULS results are compared with FEM results, chain lines with two dots have to be compared with $\triangle$ marks in Figs.6, 8 and 10, and with $\Diamond$ marks in Figs.7, 9 and 11.

In PULS, two sets of elastic large deflection analyses are performed. One is the analysis to simulate local buckling behaviour considering the interac-

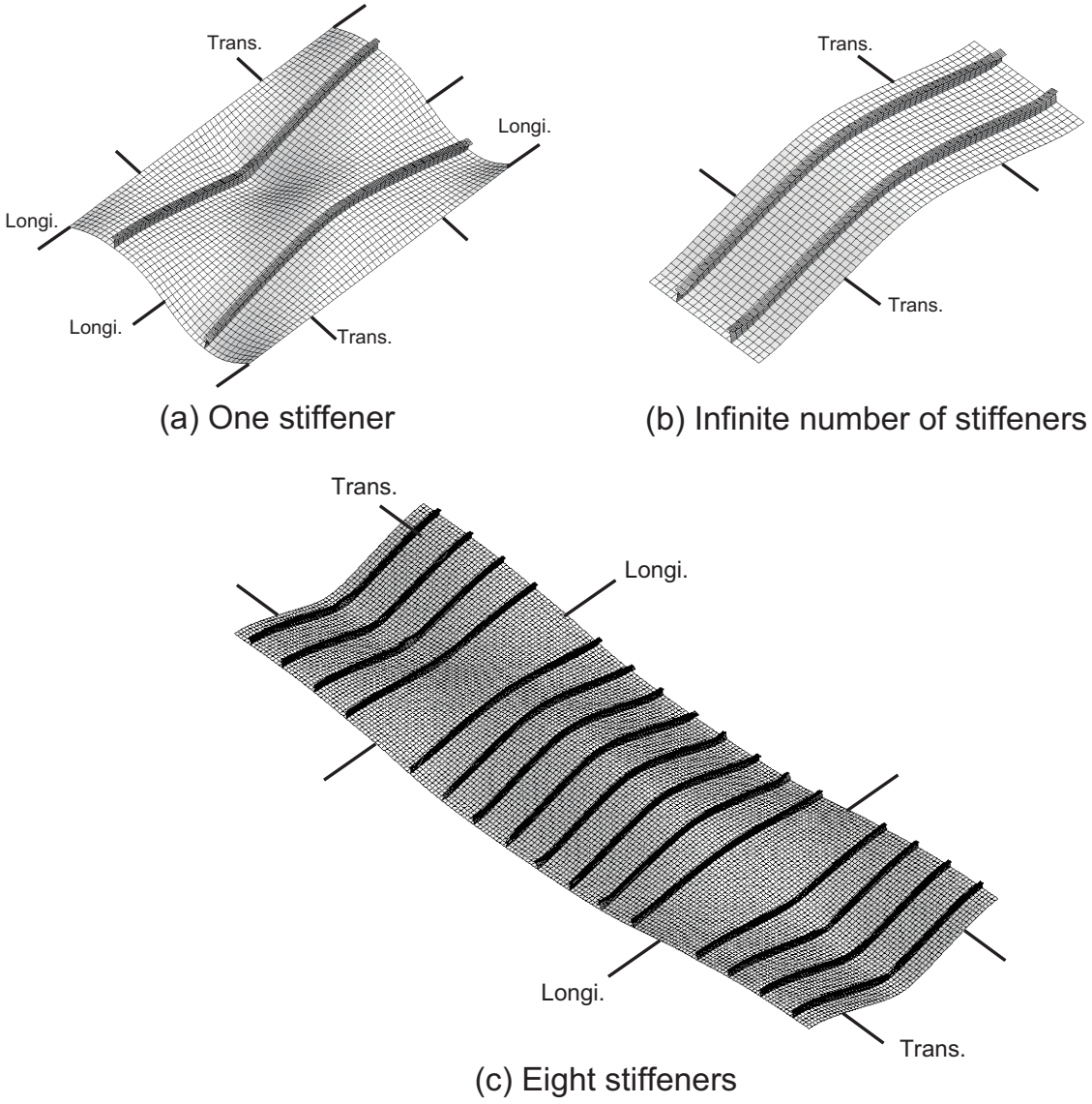

Figure 13: Typical overall collapse modes of stiffened panel (T3S1B10)

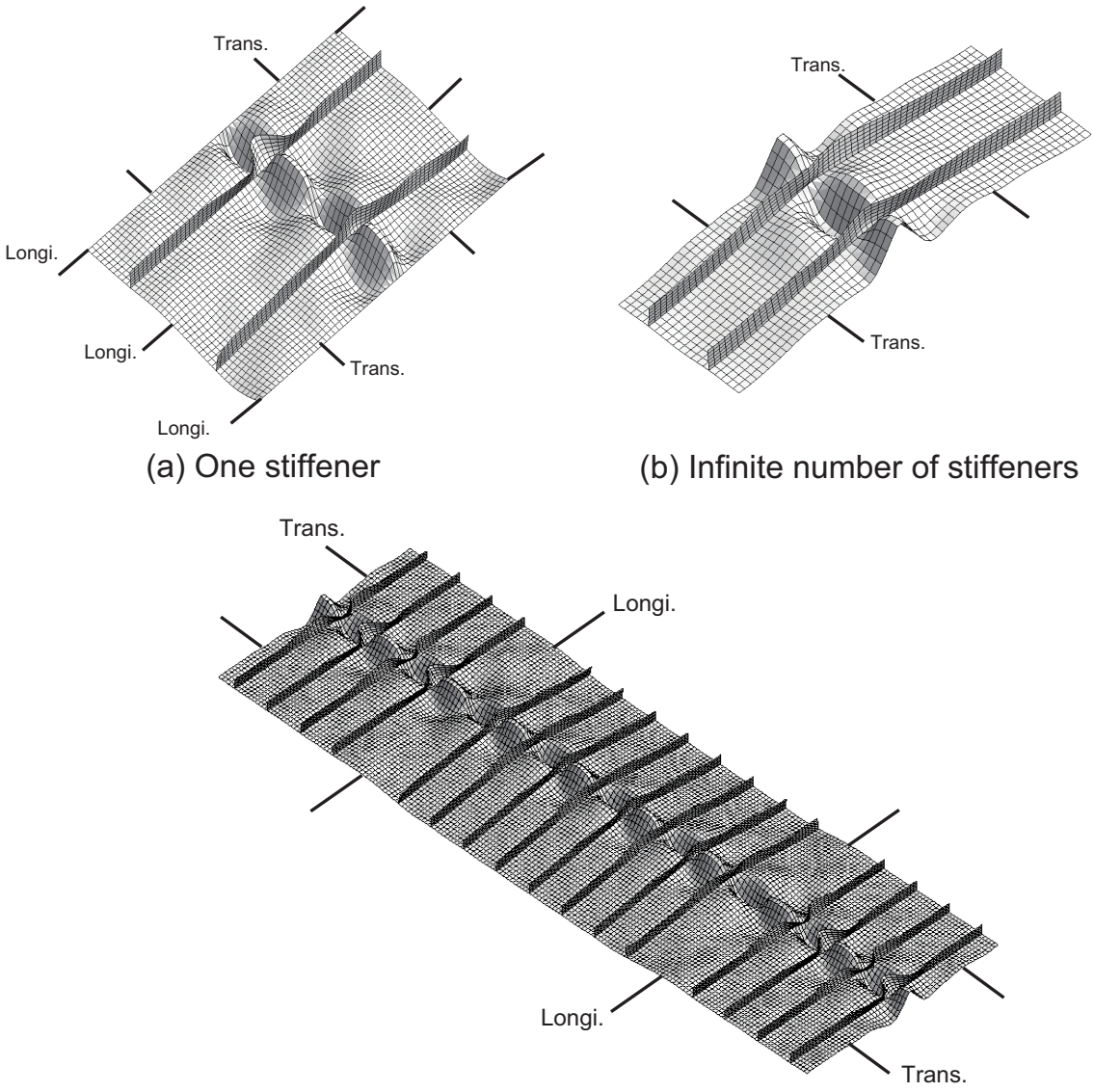

Figure 14: Typical local collapse modes of stiffened panel (F3S2B25)

tions between panel and stiffeners. Another is to simulate overall buckling behaviour replacing the stiffened panel by an orthotropic plate with equivalent flexural rigidity. The above two analyses are performed independently, although reduction in the stiffness of local panel beyond its local buckling between longitudinal stiffeners is considered when local buckling occurs before the occurrence of overall buckling. The stress components at several specified points are calculated for each model. Then, equivalent stresses are calculated with the stress components composed of membrane stresses in the local buckling model and bending stresses in the overall buckling model. The ultimate strength is determined as the lowest initial yielding strength at one of the specified points [11 - 14].

In general, the ultimate strength by PULS shows good correlation with the FEM results for stiffened panels with finite number of stiffeners under longitudinal thrust. To investigate into the accuracy of calculated results in more detail, the ratios of the ultimate strength obtained by PULS to that obtained by nonlinear FEM are examined. Calculated ratios are plotted with various marks in Figs.15 (a) through (f) which correspond to Figs.6 through 11. On the other hand, dashed lines with diamonds and solid lines with circles are the results by FY method and modified FYH formulas, respectively, which shall be explained later.

Except the cases with Size 1 stiffeners, PULS gives relatively accurate ultimate strength as the stiffener size increases. It is also known in this case that PULS underestimates the ultimate strength when slenderness ratio of the local panel is lower, while it overestimates the ultimate strength when the slenderness ratio is higher. The overestimation in case of higher slenderness ratio of local panel and larger stiffeners may come from the assumption in PULS that the number of half-waves in stiffener tripping mode is taken not as one but the same as that of local panel buckling mode.

The ultimate strength is not well predicted when one or two stiffeners of which size is small (S1 or S2) are provided and the occurrence of overall buckling dominates the collapse behaviour. This is somewhat strange since the overall buckling is accounted in the formulation of PULS regardless of the size and the number of stiffeners. The possible cause may be in the difference between buckling/plastic collapse behaviour in actual stiffened panel and its orthotropic plate model. It should also be noticed that

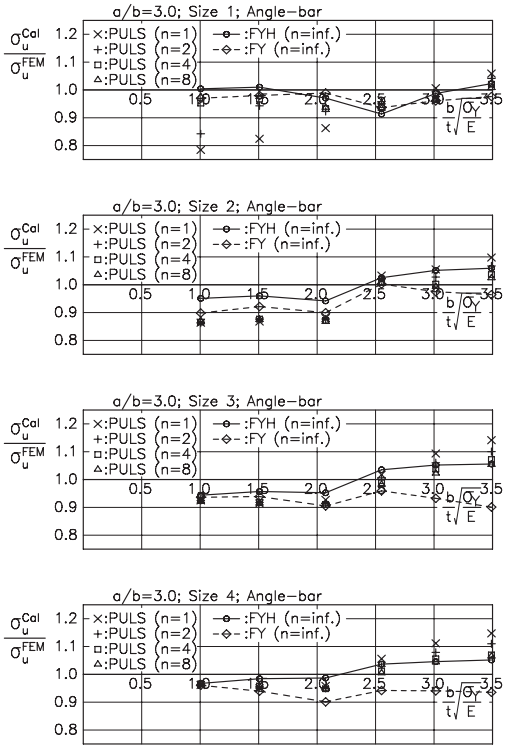

(a) Angle-bar stiffener; aspect ratio of 3.0

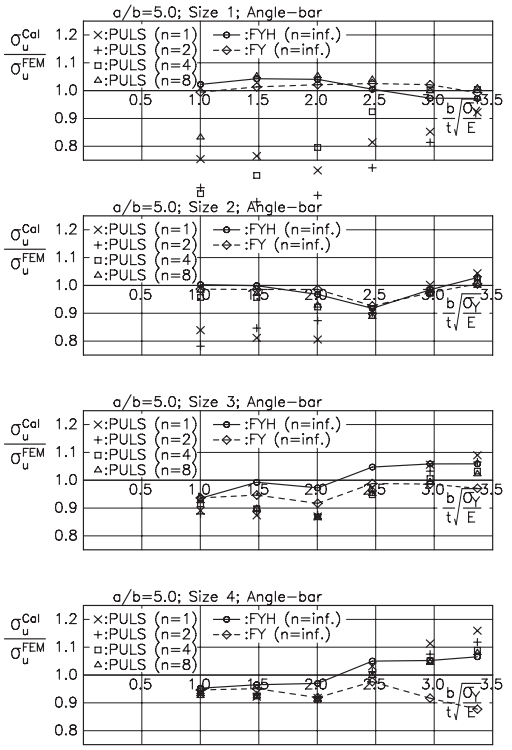

(b) Angle-bar stiffener; aspect ratio of 5.0

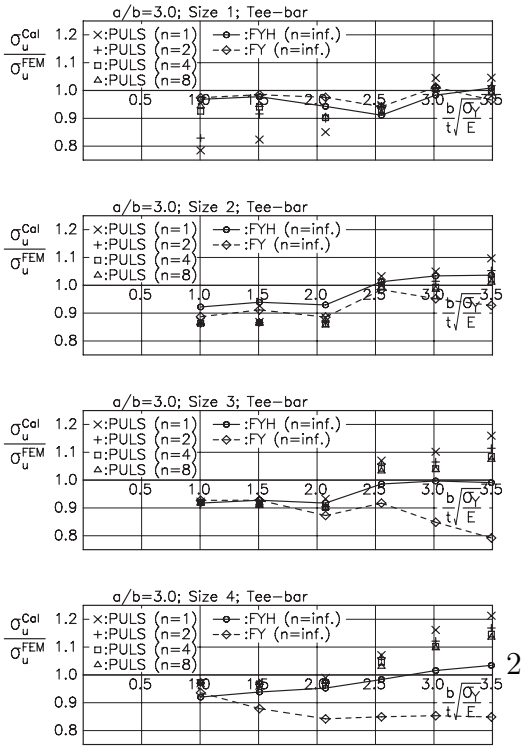

(c) Tee-bar stiffener; aspect ratio of 3.0

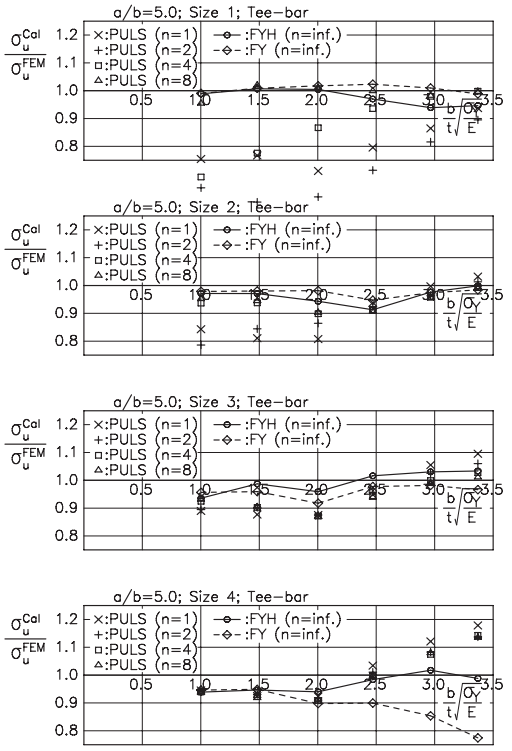

(d) Tee-bar stiffener; aspect ratio of 5.0

Figure 15: Accuracy of evaluated ultimate strength by PULS and FY method, FYH formulas

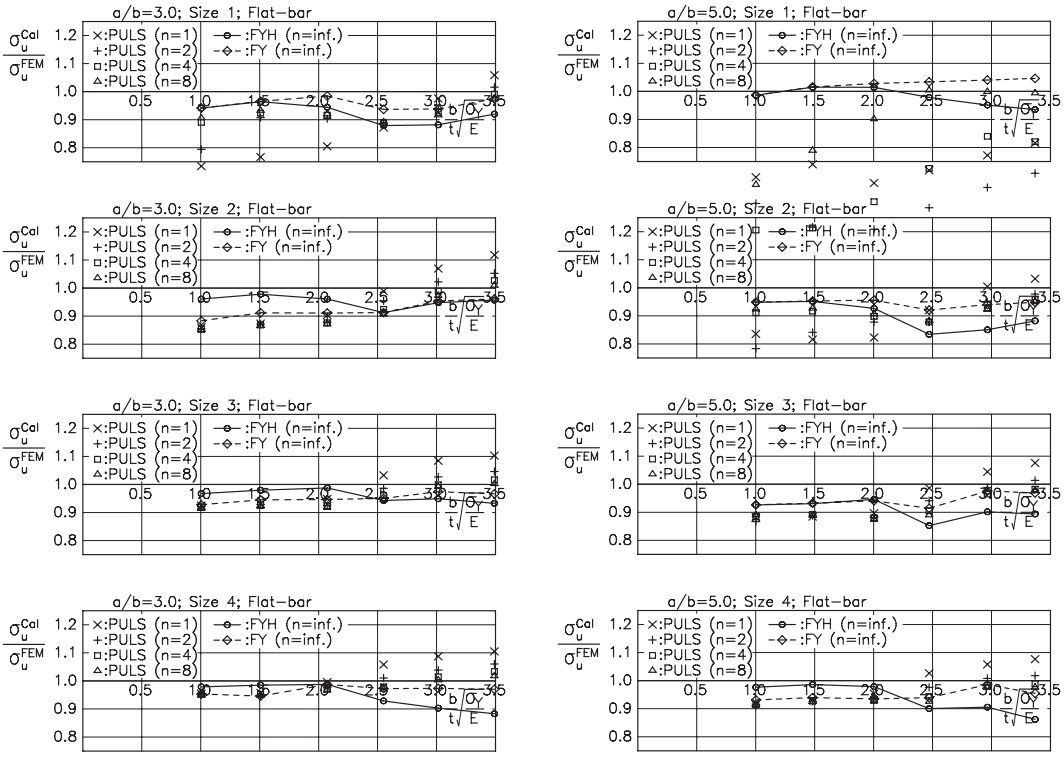

(e) Flat-bar stiffener; aspect ratio of 3.0 (f) Flat-bar stiffener; aspect ratio of 5.0

Figure 15: Accuracy of evaluated ultimate strength by PULS and FY method, FYH formulas (continued)

the ultimate strength evaluated as the initial yielding strength is, from its nature, an underestimation. The average stress-average strain and average stress-deflection relationships may be well simulated by the orthotropic plate model, but the bending stress calculated by orthotropic plate model could be a little different from the bending stress in actual stiffened panel. Any way, PULS code is fundamentally a black box for users and the real cause is not clear although its fundamental idea can be seen in Refs.[11-14]. It should be noted that PULS code is for predicting a design limit based on ultimate capacity assessment in combination with other criteria such as ensuring robust stiffeners and preventing major plastic yielding/permanent sets.

3.3. Ultimate strength by CSR-B

The ultimate strength evaluated by CSR-B [8] is plotted by chain lines with a dot in Figs.6 through 11. In CSR-B, three ultimate strength formulas are given which correspond to the collapse of local panel between longitudinal stiffeners, overall buckling collapse of a whole stiffened panel and torsional buckling collapse of stiffeners, respectively. Among the three ultimate strengths, the lowest is considered to give the real ultimate strength. For the present models, the ultimate strength formula for the collapse of local panel between longitudinal stiffeners gives the lowest value in many cases.

In general, CSR-B is said to give lower ultimate strength compared to the FEM results especially when slenderness ratio of the local panel between stiffeners is high (thinner panels). Such tendency is observed also in the present results calculated by CSR-B in Figs.6 through 11.

3.4. FY method to evaluate ultimate strength

Fujikubo *et al.*[15, 16] proposed a simple method to evaluate the ultimate strength of stiffened panel subjected to longitudinal thrust. Their method is extended for stiffened panel subjected to combined bi-axial thrust and lateral pressure [17 - 21]. However, in the present paper, fundamental idea of this method for only longitudinal thrust is briefly introduced. It is implicitly assumed that local panel can firstly buckle before overall buckllling of the stiffened panel takes place. In this case, overall buckling is considered to occur as the secondary buckling after the occurrence of local panel buckling.

In FY method, continuous stiffened panel with many stiffeners is considered, which is modelled as a beam-column composed of a stiffener and attached plating as indicated in Fig.16. The ultimate strength is determined as the lowest initial yielding strength at seven points specified in Fig.16. The initial yielding takes place when the model starts to undergo overall buckling as the secondary buckling. This behaviour is simulated by performing elastic large deflection analysis. The initial yielding is considered to occur when overall buckling takes place as the secondary buckling after local buckling. However, FY method can evaluate the ultimate strength also in the case when overall buckling firstly takes place as the primary buckling. The initial yielding strength is obtained from the following condition:

$$\Gamma = \sigma_Y - (\sigma_P + \sigma_B + \sigma_{BT} + \sigma_{WRS}) = 0 \tag{16}$$

where

$$\begin{cases} \sigma_Y & \text{(yield stress of material)} \\ \sigma_P = \dfrac{P}{A_e} & \text{(axial stress)} \\ \sigma_B = -\dfrac{M_y z}{I_y} & \text{(bending stress)} \\ \sigma_{BT} = Ey'(z'_c - z'_s)\dfrac{\mathrm{d}^2}{\mathrm{d}x^2}(\phi - \phi_0) & \text{(warping stress)} \\ \sigma_{WRS} & \text{(welding residual stress)} \end{cases} \tag{17}$$

In Eq.(17), P, M_y, I_y and A_e are axial force, vertical bending moment, second moment of inertia around horizontal neutral axis of the effective cross-section and effective cross-sectional area. ϕ and ϕ_o are total and initial twisting angle of the cross-section represented as follow.

$$\begin{aligned} \phi_0 &= \Phi_0 \sin(\pi x/a) \\ \phi &= \frac{\Phi_0}{1 - P/P_{crt}} \sin(\pi x/a) \end{aligned} \tag{18}$$

where Φ_0 is coefficient of torsional angle and P_{crt} is torsional buckling load, which is given in Appendix 2. The origin of x-coordinate is located at point B in Fig.16. In flat-bar stiffeners, warping stress (σ_{BT}) is not considered. Other parameters are given in Fig.17.

Following assumptions are made in FY method:

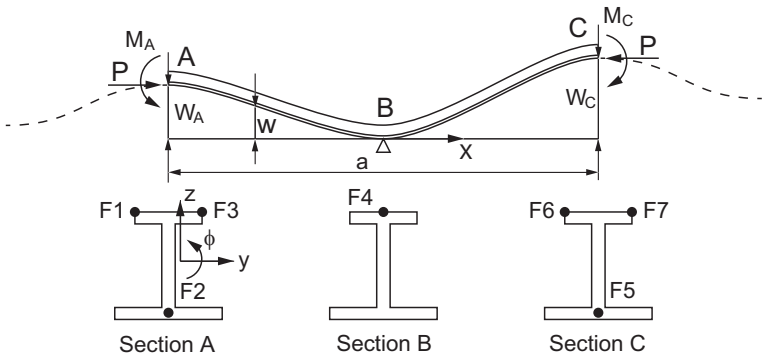

Figure 16: Double span beam-column model for stiffened panel

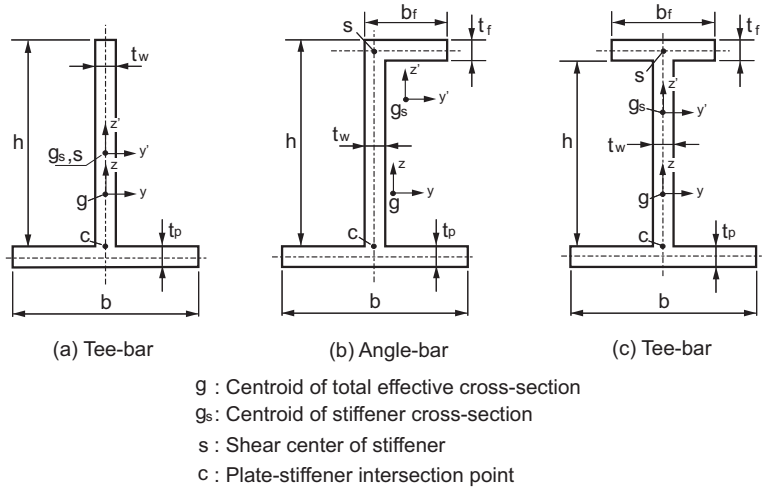

Figure 17: Cross-sections of stiffeners and their details

(1) Load-deflection and load-rotation angle relationships are assumed to be independent each other, although interactive flexural-torsional buckling is assumed to take place in case of an angle-bar stiffener.
(2) Effective width of plating beyond its local buckling is assumed constant towards the longitudinal direction.
(3) Vertical and horizontal deflections are assumed to be symmetric with respect to mid-span points.
(4) To avoid complex derivation, average strains in panel and stiffener are considered the same when effective width and effectice thickness are calculated assuming that lateral deflection at the ultimate strength is small. For the elastic large deflection analysis, this assumption is removed.

Firstly, elastic buckling stress, σ^p_{ecr}, of a local panel between stiffeners is calculated considering the interaction between panel and stiffener web in accordance with the method proposed by Fujikubo and Yao [30]. The elasto-plastic buckling stress, σ^p_{cr}, considering the influence of initial deflection is calculated with the following formula:

$$\frac{\sigma^p_{cr}}{\sigma_Y} = \frac{1}{2}\left\{ \frac{\sigma^p_{ecr}}{\sigma_Y} + 1 - \sqrt{\left(\frac{\sigma^p_{ecr}}{\sigma_Y} - 1\right)^2 + \Delta} \right\} \tag{19}$$

where σ^p_{ecr} is the elastic buckling stress considering the interaction between local panel and stiffener web.

Buckling strength calculated by Eq.(19) is shown in Fig.18 for two cases of $\Delta = 0.01$ and 0.25. It is seen that buckling strength becomes higher compared to the ordinary elastoplastic buckling strength by Johnson-Ostenfeld correction when plate is thick. For calculation by FY method in the present paper, Δ is taken as 0.25.

Then, the effective width, b_e, beyond local buckling of panel is derived as follows.

$$\frac{b_e}{b} = \begin{cases} \dfrac{\alpha_p P + (1-\alpha_p) A_s \sigma^p_{cr}}{P - (1-\alpha_p) A_p \sigma^p_{cr}} \le 1.0 & (\text{angle/tee} - \text{bar}) \\ \dfrac{\alpha_p P - (\alpha_p - \alpha_s) A_s \sigma^p_{cr}}{P - \{(1-\alpha_p) A_p + (1-\alpha_s) A_s\} \sigma^p_{cr}} \le 1.0 & (\text{flat} - \text{bar}) \end{cases} \tag{20}$$

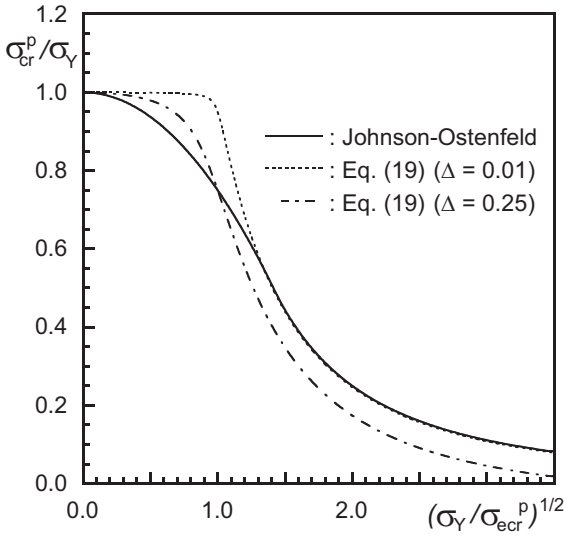

Figure 18: Elastoplastic buckling strength of local panel in stiffened panel

In case of stiffened panels with flat-bar stiffeners, flat-bar stiffener deflects in a horizontal direction when panel undergoes local buckling. The occurrence of horizontal deflection reduces the axial stiffness of the stiffener. Such phenomenon is simulated by introducing effective thickness of stiffener web panel instead of reducing the web height (effective width). Effective thickness, t_e, is expressed as:

$$\frac{t_e}{t_w} = \frac{\alpha_s P + (\alpha_p - \alpha_s) A_p \sigma_{cr}^p}{P - \{(1-\alpha_p)A_p + (1-\alpha_s)A_s\}\sigma_{cr}^p} \leq 1.0 \tag{21}$$

where

$$\begin{cases} \alpha_p = \dfrac{1 + (a/mb)^4}{3 + (a/mb)^4} \\ \alpha_s = \dfrac{1 + (32/45)(m\pi h/a)^4}{1 + (8/45)(4 + 5\eta^2)(m\pi h/a)^4} \end{cases} \tag{22}$$

and

$$\eta = 12 \left\{ 10 \frac{h}{b} \left(\frac{t_p}{t_w} \right)^3 - 0.3 \right\}^3 + 0.324 \leq 1.0 \tag{23}$$

η defined by Eq.(23) is a parameter to adjust the effective thickness of a flat-bar stiffener in accordance with its torsional stiffness. Eq.(23) is an empirical formula based on the results of FEM analyses to get better agreement

between the calculated and the predicted ultimate strength [16]. The detail for derivations of Eqs.(20) through (22) are given in Appendix 1.

From the assumption (3), shear forces at mid-span points (A and C in Fig.16) are zero, and consequently the reaction force at supporting point (B in Fig.16) becomes zero. Thus, the equilibrium equation for bending is expressed as:

$$EI_y \frac{\mathrm{d}^2(w - w_{0s})}{\mathrm{d}x^2} = -(Pw - Pw_A + M_A) \tag{24}$$

where

E:	Young's modulus of material
I_y:	second moment of inertia of cross-section around neutral axis
P:	axial load
M_A:	bending moment at mid-span point A
w_A:	vertical deflection at mid-span point A
w:	vertical deflection at x
w_{s0}:	vertical initial deflection at x

Different modes/magnitudes can be assumed as initial deflection in adjacent spans, that is:

$$w_{0s} = \begin{cases} -W_{0s1} \sin \dfrac{\pi x}{a} & x \leq 0 \\ \\ W_{0s2} \sin \dfrac{\pi x}{a} & x \geq 0 \end{cases} \tag{25}$$

When - $W_{0s1} = W_{0s2}$, initial deflection is in a flexural buckling mode of a both-ends simply supported column.

Then, Eq.(24) is solved considering boundary conditions at points A, B and C as follows:

(1) Deflection is zero at point B;
(2) Slope is continuous at point B;
(3) Deflection is symmetry at points A and C.

Consequently, bending moments at points A, B and C are derived as:

$$\begin{cases} M_A = \dfrac{P}{1-P/P_{crb}}\left(W_{0s1} - \dfrac{W_{0s1}+W_{0s2}}{\pi}\dfrac{\alpha}{\sin\alpha}\right) \\ M_B = \dfrac{P}{1-P/P_{crb}}\dfrac{W_{0s1}+W_{0s2}}{\pi}\dfrac{\alpha}{\tan\alpha} \\ M_C = \dfrac{P}{1-P/P_{crb}}\left(W_{0s2} - \dfrac{W_{0s1}+W_{0s2}}{\pi}\dfrac{\alpha}{\sin\alpha}\right) \end{cases} \tag{26}$$

where $\alpha = (\pi/2)\sqrt{P/P_{crb}}$ and P_{crb} represents the buckling load of a both ends simply supported column, which is given in Appendix 2.

The ultimate strength evaluated by FY method is plotted by broken lines in Figs.6 through 11. The ultimate strength by FY method divided by that obtained by nonlinear FEM analysis is plotted by dashed lines with diamonds in Fig.15. FY method gives relatively good estimation of the ultimate strength in the lower side except in the case of $a/b = 5.0$ and Size 1 stiffeners are provided. On the other hand, when tee-bar stiffeners of large size are provided, the ultimate strength is a little underestimated. This is because torsional stress is overestimated in this case. Nevertheless, it can be said that FY method fundamentally gives better estimation of the ultimate strength than PULS in many cases.

3.5. FYH formulas to evaluate ultimate strength of stiffened panels

At the end, ultimate strength obtained by FYH formulas are examined. FYH formulas [17, 18, 21] were derived on the basis of FY method [15, 16].

In FY method, iterative calculation is required to obtain initial yielding strength as the ultimate strength. Harada [17] introduced some assumptions to derive closed-form formulas to evaluate the ultimate strength of stiffened panel subjected to combined bi-axial thrust/tension and lateral pressures loads. The assumptions are as follows.

(1) As for the effective width, constant value is used which is the effective width when average strain reaches the yield strain.
(2) As for warping stress, constant value is used which is the warping stress when axial force is 40% of the general yielding axial force.

(3) As for buckling stress, σ^p_{ecr}, in Eq.(19), a simplified form is used which includes influences of panel-stiffener web interaction.

(4) Point of stress check is moved towards the depth direction in stiffener web according to the slenderness ratio, $\gamma = \sqrt{A\sigma_Y/P_{crb}}$, of the stiffener with attached plating. F1, F3, F4, F6 and F7 are at the flange surface when slenderness ratio is less than 0.5. However, it is changed to the centre of geometry of the stiffener cross-section without attached plating when slenderness ratio is more than 0.55. Between 0.5 and 0.55, it is linearly interpolated with respect to slenderness ratio.

(5) Effective thickness of a flat-bar stiffener was derived from a simple condition that angle between deflected stiffener web and panel is unchanged from a right angle.

Thus, the formula of a closed form is derived as:

$$\frac{\sigma_{ux}}{\sigma_Y} = \frac{A_e}{2A}\left[P_{cr}\left(\frac{1}{A_e}+\frac{1}{Z_e}W_{0s}\right)+\alpha\sigma_Y - \sqrt{\left\{P_{cr}\left(\frac{1}{A_e}+\frac{1}{Z_e}W_{0s}\right)^2+\alpha\sigma_Y\right\}^2 - 4\alpha\sigma_Y\frac{P_{cr}}{A_e}}\right] \quad (27)$$

where

$$\alpha = 1 - \frac{\sigma_w}{\sigma_Y} \quad (28)$$

Variables in Eqs.(27) and (28) are summarised in Table 4. From the fifth

Table 4: Variables necessary for ultimate strength calculation

σ_{ux}	ultimate strength (MPa)
σ_Y	yield strength (MPa)
A	cross-sectional area of stiffener (mm^2)
A_e	effective cross-sectional area of stiffener (mm^3)
Z_e	section modulus of effective cross-section (mm^3)
P_{cr}	flexural buckling load (N)
w_{0s}	magnitude of initial deflection in buckling mode (mm)
σ_w	warping stress (MPa)

assumption in FYH formulas, effective thickness of a flat-bar stiffener changes

from Eq.(21) to the following:

$$\frac{t_e}{t_w} = 1 - \frac{2\pi^2}{3}\left(\frac{h}{b}\right)^2\left(1 - \frac{b_e}{b}\right) \tag{29}$$

The ultimate strength calculated by FYH formulas is plotted by dashed lines in Figs.6 through 11. In the FYH formulas, Δ in Eq.(19) is taken as 0.01. They show good correlations with the FEM results, but underestimate the ultimate strength when higher flat-bar stiffeners are attached to slender plate.

To eliminate such disagreements, the definition of effective thickness of flat-bar stiffeners has been changed from Eq.(29) to the following:

$$\frac{t_e}{t_w} = \frac{\sigma_{cr}^p}{\sigma_Y}(1 - \alpha_s) + \alpha_s \tag{30}$$

where α_s is given by Eq.(22) setting as $\eta = 1.0$. The above equation was derived from Eq.(21) in FY method setting the axial strain, ε_s, in Eqs.(A1.13) and (A1.14) in Appendix 1 as the yield strain.

The ultimate strength calculated by modified FYH formulas is plotted by solid lines in Figs.6 through 11. At the same time, the ultimate strength divided by that of FEM results is plotted in Fig.15 by solid lines with circles. Comparison of solid and dashed lines in Fig.15 indicates that the difference between the ultimate strength by FY method and modified FYH formulas is not so large. In some cases, modified FYH formulas give lower estimation than FY method, while in other cases higher estimation. When slenderness ratio of local panel is higher and flat-bar stiffeners are provided, FYH formulas give lower ultimate strength. This could be attributed to lower estimation of the assumed effective thickness of flat-bar stiffeners.

Comparing the ultimate strength by modified FYH formulas with that by PULS, it is seen that modified FYH gives better estimations than PULS in many cases especially when smaller stiffeners are provided.

It can be concluded that FY method, modified FYH formulas and PULS give good estimation of the ultimate strength of stiffened panel under longitudinal thrust. However, it should be noticed that the modified FYH formulas

are of a closed form and are much easier to calculate the ultimate strength. This could be an advantage of FYH formulas.

4. CONCLUDING REMARKS

A series of nonlinear FEM analyses is performed on 720 stiffened panels under longitudinal thrust varying the numbers, types and sizes of stiffeners as well as aspect ratio and slenderness ratio of local panels partitioned by stiffeners. The spacing between adjacent longitudinal girders is kept the same. It has been found that:

1. When smaller stiffeners are attached to thicker panel, occurrence of overall buckling dominates the collapse behaviour, and the ultimate strength largely differs depending on the number of stiffeners and so the aspect ratio of the whole stiffened panel.
2. When larger stiffeners are provided, occurrence of collapse of the local panels paritioned by stiffeners dominates the collapseb behaviour, and the collapse behaviour and the ultimate strength are almost the same regardless of the number of stiffeners.
3. The ultimate strength of stiffened panel under longitudinal thrust evaluated by CSR-B is in general lower compared to that evaluated by nonlinear FEM analysis.
4. Fujikubo/Yanagihara (FY) method, modified Fujikubo/Yanagihara /Harada (FYH) formulas and PULS give relatively accurate ultimate strength of stiffened panel under longitudinal thrust.
5. Among the above three, modified FYH formulas are of a closed form, and are considered the best.

5. ACKNOWLEDGEMENTS

This research was partially supported by the Ministry of Education, Science, Sports and Culture, through Grant-in-Aid for Young Scientists (B) (21760668).

Appendix 1: Derivation of Effective Width

The buckling mode of simply supported panel under longitudinal thrust can be assumed as:

$$w = W \sin \frac{m\pi x}{a} \sin \frac{\pi y}{b} \tag{A1.1}$$

The compatibility condition of this plate with large deflection is expressed as:

$$\frac{\partial^4 F}{\partial x^4} + 2\frac{\partial^4 F}{\partial x^2 \partial y^2} + \frac{\partial^4 F}{\partial y^4} = E\left[\left(\frac{\partial^2 w}{\partial x \partial y}\right)^2 - \left(\frac{\partial^2 w}{\partial x^2}\right)\left(\frac{\partial^2 w}{\partial y^2}\right)\right] \tag{A1.2}$$

where F in Eq.(A1.2) is Airy's stress function, and is obtained for the assumed deflection, Eq.(A1.1), as follows.

$$F = \frac{E}{32} W^2 \left(\frac{a^2}{b^2}\cos\frac{2\pi x}{a} + \frac{b^2}{a^2}\cos\frac{2\pi y}{b}\right) \tag{A1.3}$$

Applying Principle of Virtual Work, following equations are derived in terms of average stress, average strain and deflection.

$$\frac{m^2\pi^2 a^2 E}{16}\left(\frac{1}{a^4} + \frac{1}{m^4 b^4}\right) W^3 + \frac{\pi^2 t_p{}^2 E}{12(1-\nu^2)b^2}\left(\frac{a}{mb} + \frac{mb}{a}\right)^2 W - \sigma W = 0 \tag{A1.4}$$

$$\varepsilon = \frac{1}{E}\sigma + \frac{m^2\pi^2}{8a^2} W^2 \tag{A1.5}$$

Eliminating W from Eqs.(A1.4) and (A1.5), average stress-average strain relationship is derived as follows.

$$\sigma = \sigma_{cr} + \frac{1 + (a/mb)^4}{3 + (a/mb)^4} E \cdot (\varepsilon - \varepsilon_{cr}) \tag{A1.6}$$

where

$$\sigma_{cr} = \frac{\pi^2 t_p{}^2 E}{12(1-\nu^2)b^2}\left(\frac{a}{mb} + \frac{mb}{a}\right)^2, \quad \varepsilon_{cr} = \frac{1}{E}\sigma_{cr} \tag{A1.7}$$

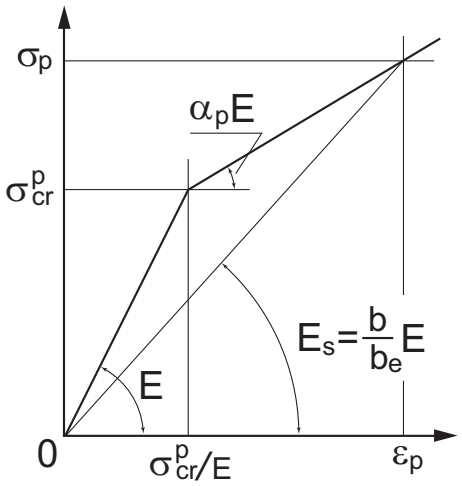

Fig.A1.1 Average stress-average strain relationship beyond buckling

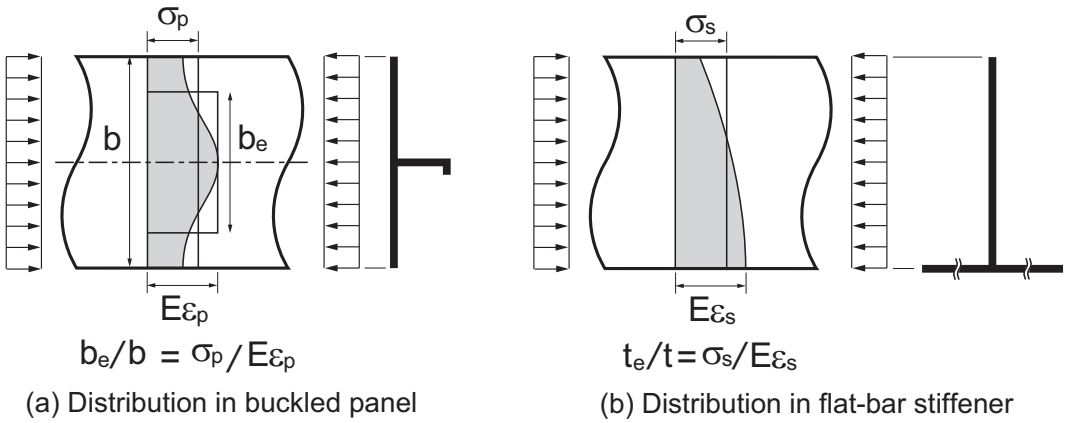

Fig.A1.2 Stress distribution beyond buckling

Eq.(A1.6) can be re-written using the same variables in the main text as:

$$\sigma_p = \sigma_{cr}^{\ p} + \alpha_p(E\varepsilon_p - \sigma_{cr}^{\ p}), \quad \alpha_p = \frac{1+(a/mb)^4}{3+(a/mb)^4} \tag{A1.8}$$

Here, effective width is considered. After the panel buckles, the average stress-average strain relationship becomes as indicated in Fig.A1.1, and the stress distribution in the panel as Fig.A1.2 (a).

The compressive load which is sustained by the panel is then expressed as:

$$P_{pl} = \sigma_p b t_p = E_s \varepsilon_p b t_p = E\varepsilon_p b_e t_p \tag{A1.9}$$

Hence,

$$\sigma_p = E_s\varepsilon_s = \frac{b_e}{b} E\varepsilon_p \tag{A1.10}$$

It is assumed that deflection of the stiffener is very small at the ultimate strength, and is assumed that axial strain in the stiffener, ε, is uniform all over the cross-section. From this assumption, the following relationship is derived.

$$P = E(b_e t_p + A_s)\varepsilon_p \tag{A1.11}$$

From Eqs.(A1.8), (A1,10) and (A1.11), effective width is derived as follows.

$$\frac{b_e}{b} = \frac{\alpha_p P + A_s(1-\alpha_p)\sigma_{cr}^{\ p}}{P - A_p(1-\alpha_p)\sigma_{cr}^{\ p}} \tag{A1.12}$$

which corresponds to the first equation of Eq.(20) in the main text.

When flat-bar stiffeners are attached, stress in the stiffener also becomes non-uniform as indicated in Fig.A1.2 (b). One method to account this influence is to reduce the height of the stiffener since the rigidity is proportional to the cube of the height. However, flexural rigidity of the flat-bar stiffener may be too much reduced. Therefore, instead of reducing web height, web thickness is reduced and effective thickness is defined as follows.

$$\sigma_s = \frac{t_e}{t_w} E\varepsilon_s \tag{A1.13}$$

Here, deflection mode with the same half-wave number with that in local panel is assumed although the boundary condition of the web plate is assumed as three sides simply supported and one side free. Thus, the average

stress-average strain relationship of the stiffener is expressed as follows.

$$\sigma_s = \sigma_{cr}^{\ p} + \alpha_s(E\varepsilon_s - \sigma_{cr}^{\ p}), \quad \alpha_s = \frac{1 + (32/45)(m\pi h/a)^4}{1 + (72/45)(m\pi h/a)^4} \tag{A1.14}$$

In Eq.(A1.14), interaction between local panel and stiffener web is considered when the buckling stress, $\sigma_{cr}^{\ p}$, is derived. α_s in Eq.(A1.14) corresponds to the second equation of Eq.(19) in the main text for the case of $\eta = 1.0$.

Here, the same assumption is made that the deflection is very small at the ultimate strength, and the stress (and so the strain) in the cross-section is uniform. Then,

$$P = E(b_e t_p + h t_e)\varepsilon_p \tag{A1.15}$$

With Eqs.(A1.12) through (A1.14) together with Eqs.(A1.8) and (A1.9), effective breadth and effective thickness of local panel and flat-bar stiffener are derived as follows.

$$\frac{b_e}{b} = \frac{\alpha_p P - (\alpha_p - \alpha_s)A_s\sigma_{cr}^{p}}{P - \{(1-\alpha_p)A_p + (1-\alpha_s)A_s\}\sigma_{cr}^{p}} \tag{A1.16}$$

$$\frac{t_e}{t_w} = \frac{\alpha_s P + (\alpha_p - \alpha_s)A_p\sigma_{cr}^{p}}{P - \{(1-\alpha_p)A_p + (1-\alpha_s)A_s\}\sigma_{cr}^{p}} \tag{A1.17}$$

These equations correspond to Eqs.(20) and (21) in the main text.

Appendix 2: Derivation of Flexural-Torsional Buckling Loads of Stiffener with Attached Plating

In the calculation of elastic buckling load of a stiffener with attached plating, it is assumed that the attached plating contributes only to the flexural buckling in the direction perpendicular to the plating.

For flat-bar and tee-bar stiffeners, flexural buckling load, P_{crb}, and torsional buckling load, P_{crt}, are independent and are given as follows.

$$P_{crb} = a_1 \tag{A2.1}$$

$$P_{crt} = a_4/(\xi a_3) \tag{A2.2}$$

In case of angle-bar stiffener, flexural-torsional buckling takes place when axial force reaches to the buckling load, P_{crbt}, which is expressed as:

$$P_{crbt} = (-b_2 + \sqrt{b_2^2 - 4b_1b_3})/(2b_1) \tag{A2.3}$$

where

$$\begin{aligned} a_1 &= \pi^2 E I_y / a^2 \\ a_2 &= \pi^2 E I'_{yz}(z'_s - z'_c)/a^2 \\ a_3 &= I'_o/A_s - z'^2_s + z'^2_c \\ a_4 &= \pi^2 E I'_z (z'_s - z'_c)^2/a^2 + C' + a^2 k_\phi/\pi^2 \\ b_1 &= \xi(\xi y'^2_s - a_3) \\ b_2 &= \xi(a_1 a_3 - 2y'_s a_2) + a_4 \\ b_3 &= a_2^2 - a_1 a_4 \end{aligned} \tag{A2.4}$$

and

$$\begin{aligned} &\xi = A_s/A_e, \quad I_y = \int z^2 \mathrm{d}A_e, \quad I'_y = \int z'^2 \mathrm{d}A_s, \\ &I'_z = \int y'^2 \mathrm{d}A_s, \quad I'_{yz} = \int y'z' \mathrm{d}A_s, \\ &I'_o = I'_y + I'_z + (y'^2_s + z'^2_s)A_s \end{aligned} \tag{A2.5}$$

A_s and A_e are the cross-sectional area of a stiffener alone and stiffener with attached plating. On the other hand, C' is Sant-Venant's torsional rigidity of a stiffener, and k_ϕ represents the resistance from the panel against rotation of the stiffener. k_ϕ is expressed as follows.

$$k_\phi = \frac{E t_p^3}{3b} \tag{A2.6}$$

In case of stiffened panels with angle-bar stiffeners, P_{crt} in Eq.(18) and P_{crb} in Eq.(26) in the main text are both replaced by P_{crbt}.

References

[1] Yao T., Fujikubo M., Mizutani K., Collapse behaviour of rectangular plates subjected to combined thrust and lateral pressure, Transactions of the West-Japan Society of Naval Architects, 1996, Vol. 92, pp. 249-262 (in Japanese).

[2] Guades Soares C., Gordo J. M., Compressive strength of rectangular plates under biaxial load and lateral pressure, Thin-Walled Structures, 1996, Vol. 24, pp. 231-259.

[3] Yao T. *et al.*, Ultimate Hull Girder Strength, Report of STC IV.2, Proceedings of 14th International Ship and Offshore Structures Congress (ISSC), 2000, Vol. 2, pp. 321-391.

[4] Paik J. K., Thayamballi A. K., Kim B. J., Large deflection orthotropic plate approach to develop ultimate strength formulations for stiffened panels under combined biaxial compression/tension and lateral pressure, Thin-Walled Structures, 2001, Vol. 39, pp. 215-246.

[5] Fujikubo M., Yao T., Elastic local buckling strength of stiffened plate considering plate/stiffener interaction and welding residual stress, 1999, Vol. 12, Marine Structures, pp. 543-564.

[6] Fujikubo M., Yao T., Khedmati M. R., Harada M., Yanagihara D., Estimation of ultimate strength of continuous stiffened panel under combined transverse thrust and lateral pressure, Part 1: Continuous plate, Marine Structures, 2005, Vol. 18, pp. 383-410.

[7] Fujikubo M., Harada M., Yao T., Khedmati M. R., Yanagihara D., Estimation of ultimate strength of continuous stiffened panel under combined transverse thrust and lateral pressure, Part 2: Continuous stiffened panel, Marine Structures, 2005, Vol. 18, pp. 411-427.

[8] IACS, Common Structural Rules for Bulk Carriers, 2006.

[9] IACS, Common Structural Rules for Double Hull Oil Tankers, 2006.

[10] Det Norske Veritas, Nauticus Hull User Manual, PULS, 2005.

[11] Byklum E., Amdahl J., A simplified method for elastic large deflection analysis of plates and stiffened panels due to local buckling, Thin-Walled Structures, 2002, Vol. 40, pp. 925-953.

[12] Byklum E., Steen E., Amdahl J., A semi-analytical model for global buckling and postbuckling analysis of stiffened panels, Thin-Walled Structures, 2004, Vol. 42, pp. 701-717.

[13] Steen E., Byklum E., Vilming K. G., Ostvold T. K., Computerized buckling models for ultimate strength assessment of stiffened ship hull panels, Proceedings of 11th Symposium On Practical Design of Ships and Other Floating Structures (PRADS), 2004, pp. 235-242.

[14] Steen E., Byklum E., Ultimate strength and postbuckling stiffness of plate panels subjected to combined loads using semi-analytical models, Proceedings of International Conference on Marine Research and Transportation (ICMRT), 2005, pp. 1-8.

[15] Fujikubo M., Yanagihara D., Yao T., Estimation of ultimate strength of continuous stiffened plates under thrust, Journal of the Society of Naval Architects of Japan, 1999, Vol. 185, pp. 203-212 (in Japanese).

[16] Fujikubo M., Yanagihara D., Yao T., Estimation of ultimate strength of continuous stiffened plates under thrust (2nd report), Journal of the Society of Naval Architects of Japan, 1999, Vol. 186, pp. 631-638 (in Japanese).

[17] Harada M., Practical method to estimate ultimate strength of members in ship structure, 2004, Dr. Thesis, Hiroshima University (in Japanese).

[18] Harada M., Fujikubo M., Yanagihara D., Development of simple formulae of ultimate strength of continuous stiffened plates under combined thrust and lateral pressure, Journal of the Kansai Society of Naval Architects, Japan, 2004, Vol. 241, pp. 159-168 (in Japanese).

[19] Harada M., Fujikubo M., Yanagihara D., Development of a set of simple formulae for estimation of ultimate strength of a continuous stiffened panel under combined loads, Journal of the Japan Society of Naval Architects and Ocean Engineers, 2005, Vol. 2, pp. 387-395 (in Japanese).

[20] Harada M., Fujikubo M., Yanagihara D., Estimation of ultimate strength of continuous stiffened plate under combined biaxial thrust and lateral pressure, Journal of the Society of Naval Architects of Japan, 2004, Vol. 196, pp. 189-198. (in Japanese)

[21] Harada M., Fujikubo M., Yanagihara D., Development of a set of closed-form formulae for estimation of ultimate strength of a continuous stiffened panel under combined in-plane loads and lateral pressure, ClassNK Technical Bulletin, 2007, Vol. 25, pp. 11-21.

[22] MSC.Marc 2005r3, User's Guide.

[23] Yao T., Fujikubo M., Yanagihara D., Irisawa M., Considerations on FEM modeling for buckling/plastic collapse analysis of stiffened plates,

The West-Japan Society of Naval Architects, 1998, Vol. 95, pp. 121-128 (in Japanese).

[24] Xu M. C., Yanagihara D., Fujikubo M., Guedes Soares C., Influence of boundary conditions on the collapse behaviour of stiffened panels under combined loads, Marine Structures, 2013, Vol. 34, pp. 205-225.

[25] The Japan Society of Naval Architects and Ocean Engineers: Report of Research Committee for Verification of ISO Formulas to Evaluate Ultimate Strength, 2011.

[26] Ueda Y., Yao T., The influence of complex initial deflection modes on the behaviour and ultimate strength of rectangular plates in compression, Journal of Constructional Steel Research, 1985, Vol. 5, pp. 265-302.

[27] Yao T., Fujikubo M., Yanagihara D., Varghese B., Niho O., Influences of welding imperfections on buckling/ultimate strength of ship bottom plating subjected to combined bi-axial thrust and lateral pressure, Proc. Int. Symp. Thin-Walled Structures, Singapore, 1998, pp.425-432.

[28] Smith C. S., Davidson P. C., Chapman J. C., Dowling P. J., Strength and stiffness of ship plating under in-plane compression and tension, Transactions of RINA, 1987, Vol. 130, pp. 277-296.

[29] Research committee on steel ship construction: Japan Shipbuilding Quality Standars (JSQS), Society of Naval Architects, Japan, 1979, p. 28.

[30] Fujikubo M., Yao T., Elastic local buckling strength of stiffened plate considering plate/stiffener interaction and welding residual stress, Marine Structures, 1999, Vol.12, pp.543-564.